A comparison between flume and field bedload transport data and consequences for surface-based bedload transport prediction

A. Recking

A comparison between flume and field bedload transport data and consequences for surface-based bedload transport prediction

A. Recking, Researcher, Cemagref, UR Erosion Torrentielle Neige Avalanches, 2 rue de la papeterie, BP76, 38402 Saint Martin d'Hères, France. E-mail: alain.recking@cemagref.fr

ABSTRACT

The ability of simple equations to predict bedload transport with limited knowledge of the bed surface material was investigated. This was done using a data set consisting of 7,636 bedload transport values from the flume (1,317 data) and from 84 river reaches (6,319 field data). It was possible to collapse field and flume data by correcting the ratio between the Shields number and its critical value with a very simple hiding function proposed as a power law of the D_{84}/D_{50} ratio. Doing so, a surface-based bedload transport formula was proposed. It was successfully tested on an independent data set (comprising sand and gravel bed rivers with slope in the range 0.0002–0.08), with 86% of the values predicted within a precision of one order of magnitude. Moreover, the formula reproduced the low transport rates well, contrary to the usual surface-based formulas also tested, and is particularly well suited for estimating low transport rates associated with near bankfull flow discharge. This new formula is neither time- (no fractionwise calculation) nor data-consuming (the required parameters are the flow discharge, the active width, the slope, and the surface grain diameters D_{50} and D_{84}).

INTRODUCTION

Bedload prediction is of primary importance for river engineering, fluvial geomorphology, eco-hydrology, environmental surveys and management, and hazard prediction. Many well-known bedload equations were partly (if not totally) derived from flume experiments using uniform sediments [*Meyer-Peter and Mueller*, 1948; *Schoklitsch*, 1962; *Parker*, 1979; *Rickenmann*, 1991]. In such conditions, equations based on the unique grain diameter D permit a fair representation of complex feedback between friction, tractive forces, and transport [*Recking et al.*, 2008b]. There have been several attempts to adapt these equations to rivers, and the results indicate that, especially when gravel-bed rivers are considered, they usually under- or overpredict the observed bedload transport by several orders of magnitude [*Bathurst et al.*, 1987; *Gomez and Church*, 1989; *Cardoso and Neves*, 1994; *Molinas and Wu*, 1998; *Yang and Huang*, 2001; *Almedeij and Diplas*, 2003; *Bravo-Espinosa et al.*, 2003; *Martin*, 2003; *Barry et al.*, 2004; *Pitlick et al.*, 2008].

One major difficulty in applying these formulas is that in gravel-bed rivers, sediments are poorly sorted and that consequently, the choice of a characteristic grain size D_i (the size such that i% is finer) to be used in place of the uniform grain size D is not trivial. Indeed, in the field many events correspond to partial transport, with fine sediments being transported, whereas coarser ones are maintained at rest [*Wilcock and McArdell*, 1993]. In addition, because of hiding effects altering the shear stress acting on fine sediments [*Einstein and Chien*, 1953; *Egiazaroff*, 1965], the same flow condition and the same representative diameter D_{i} will not necessarily produce the same transport rate when different sediment size gradations are used [*Molinas and Wu*, 1998]. This explains why equations based on the transport threshold of a unique given bed surface diameter usually exhibit poor performance, because they consider that no transport is possible as long as this diameter is at rest, and by

doing so, they underestimate low transport rates of fine particles [*Barry et al.*, 2004]. Very sophisticated models were developed that take into account these effects by calculating a fractional-based bedload transport, i.e., a calculation size by size [*Parker*, 1990; *Wilcock and Crowe*, 2003]. In practice, these models are difficult to use because information concerning the complete surface grain size distribution is rare. This explains why simple models, based on a single characteristic grain size, continue to be widely used in field applications, even though it is generally recognized that they have very limited efficiency for typical flow events in gravel-bed rivers with poorly sorted sediments. Therefore, there is a real need to investigate further the ability of simple equations to predict mean bedload transport with limited knowledge of the bed surface material. This paper aims to investigate whether recently published extensive bedload transport data sets [*King et al.*, 2004] and results on bedload and flow resistance modeling [*Recking et al.*, 2008b] and critical Shields stress [*Recking*, 2009] can help to improve bedload prediction with such simple models.

In many rivers with coarse bed material, the sediment supplied is stored vertically in a coarse fraction that is retained on the bed surface, i.e., the armor layer, and a fine fraction that goes into temporary storage in the bed, i.e., the substrate [*Pitlick et al.*, 2008]. A different transport phase can be considered regarding the armor mobility [*Jackson and Beschta*, 1982; *Ashworth and Ferguson*, 1989; *Ryan et al.*, 2002; *Bathurst*, 2007]: as long as the threshold for break-up of the armor layer is not attained, phase 1 is considered, with bedload composed of fine sediments supplied from upstream or from patches of fine materials and passing over the immobile armor layer. When the flow condition permits the break-up of the armor, phase 2 is considered where coarse grains can participate in transport and the availability of fine sediments from the subsurface is increased [*Parker et al.*, 1982]. To finish, a phase 3 can also be considered once all sizes are in motion [*Parker et al.*, 1982; *Wilcock and McArdell*, 1993].

A model should be able to reproduce all these transport phases. To attain this objective, and considering the role of the armor, this paper proposes to relate transport rates to the mobility of the bed armor. Thus, calculations will be performed in relation to the threshold conditions of a characteristic grain size representative of the bed armor only, instead of considering the entire surface (or sub-surface) sediment mixture as is usually done. Moreover, because of hiding effects, several transport rates can exist for a given characteristic grain size and flow condition and, consequently, at least two parameters should be defined before deriving a bedload equation: a characteristic grain size and a sorting coefficient.

Recently published results and the data sets are presented first. Secondly, the bedload equation is developed using 3,200 bedload values measured in Idaho rivers [*King et al.*, 2004]. Third, the model is tested on an additional data set comprising 3,119 field bedload values from the literature. Finally, the consequences of this study for bedload prediction are presented and discussed. All analyses were performed with comparisons with bedload transport of uniform sediments (1,317 flume values) already analyzed in *Recking et al.* [2008b].

SUMMARY OF PREVIOUS STUDIES AND DATA SETS

Summary of previous results

Since hydraulic parameters (mean velocity U and flow depth H) are often unknown or can be associated with large uncertainties, the procedure developed in this study directly calculates the hydraulic radius R from the flow discharge Q (measured at the gauging station). The following flow resistance equation (deduced from the analyses of 2282 flume and field values in *Recking et al.* [2008b]) is used:

$$\frac{U}{\sqrt{gRS}} = 6.25 + 5.75\log\left(\frac{R}{\alpha_{RL}\alpha_{BR}D}\right) \quad (1)$$

With $\alpha_{RL} = 4\left(\frac{R}{D}\right)^{-0.43}$ with $1 \le \alpha_{RL} \le 3.5$

$$\alpha_{BR} = 7S^{0.85}\frac{R}{D} \text{ with } 1 < \alpha_{BR} \le 2.6$$

where U is the vertically averaged flow velocity, α_{RL} is a roughness layer coefficient taking into account deviation from the logarithmic profile on small relative depth flows (with an increasing influence of the roughness layer), and α_{BR} is a bedload roughness coefficient taking into account additional flow resistance caused by bedload. This equation was initially derived for flat bed conditions obtained with uniform sediments in flume experiments and was representative of the grain resistance only. However, it was also successfully tested on mean flow velocities measured in the field when D was replaced by D_{84}. Used with the mass conservation equation ($Q=WHU$), this equation calculates the flow hydraulic radius R and the shear stress ($\tau=\rho gRS$). This approach should be a good approximation when the flow can be considered nearly uniform at the reach scale (in other conditions and for flows over dunes, the measured flow velocity U or depth H might be necessary for the grain shear stress estimate).

The bedload data of uniform sediments was composed of 1,317 values (see auxiliary material) described in Table 1 and plotted in Figure 1a). They were analyzed by *Recking et al.* [2008b] and will be used for comparison with field data throughout this paper. Transport of uniform sediments was associated with two transport phases [*Recking et al.*, 2008a], with a low transport rate corresponding to partially mobile grains and a high transport rate corresponding to fully mobile grains. These two transport phases are not identical to phase 1 and phase 2 described in the introduction, as there was no armor layer regulating the release of fine sediments in these experiments (they may instead correspond to phases 2 and 3 in the

introduction). It was necessary to vary the critical Shields stress θ_c with the slope S in order to fit the low transport rate data, whereas the high transport rate data were adequately fitted with a power law, with no dependence on the critical Shields stress [*Recking et al.*, 2008b]:

$$\Phi = 15.6(\theta - \theta_c)^2 \qquad \text{if } \theta < 0.65S^{0.41}$$

$$\Phi = 14\theta^{2.45} \qquad \text{if } \theta > 0.65S^{0.41} \tag{2}$$

where $\Phi=q_{sv}/[g(s\text{-}1)D^3]^{0.5}$ is the Einstein dimensionless parameter [*Einstein*, 1950], q_{sv} [$m^3/s/m$] is the volumetric unit solid discharge, $\theta=\tau/(g[\rho_s\text{-}\rho]D)=RS/([D(s\text{-}1)]$ is the Shields number, R is the flow hydraulic radius, $s = \rho_s/\rho$ is the sediment relative density, ρ_s is the sediment density, and ρ is the water density. The critical Shields number θ_c was given as a function of the slope S:

$$\theta_c = 0.15S^{0.275} \tag{3}$$

The flow resistance equation (Eq. 1) was used to derive a velocity profile equation incorporating a roughness layer in *Recking* [2009]. When included in a force balance model, this velocity profile adequately reproduced the variation of the critical Shields stress with the slope (Eq. 3). A critical Shields stress function fitted on field data [*Recking*, 2009] will also be considered in this study:

$$\theta_{ci} = (1.32S + 0.037)\left(\frac{D_i}{D_{50}}\right)^{-0.93} \tag{4}$$

where D_{50} is the median grain size, θ_{ci} is the critical Shields stress relative to diameter D_i, and D_i is the size for which i% of the particle size distribution is finer. Another recently published papers described a critical Shields stress increase with increasing slope [*Mueller et al.*, 2005; *Lamb et al.*, 2008].

In order to facilitate a comparison between uniform and nonuniform sediment, the uniform sediment data set was plotted as a function of the θ/θ_c ratio (using Eq. 3 for θ_c) in Figure 1b.

The results indicate that the use of θ/θ_c can collapse the data for the low transport rate but conversely increases the scatter for the high transport rate (for which we previously observed no dependence on θ_c). The resulting equation is:

$$\Phi = 0.00005\left(\frac{\theta}{\theta_c}\right)^{12.9} \quad \text{for } \theta/\theta_c < 2.3S^{0.08}$$
$$\Phi = 14\theta^{2.45} \quad \text{for } \theta/\theta_c > 2.3S^{0.08} \tag{5}$$

This equation applies to uniform sediments and will be used for comparison with field data.

Data sets

The data set used to investigate a bedload equation is made up of 3,200 field bedload transport values from 33 Idaho streams and rivers [*King et al.*, 2004]. These data have already been analyzed in several papers [*Barry et al.*, 2004; *Mueller et al.*, 2005; *Barry et al.*, 2008; *Muskatirovic*, 2008; *Pitlick et al.*, 2008]. Slopes at the study sites range from 0.0003 to 0.07, bankfull depths range from 0.2 to 5 m, bankfull widths range from 2 to 200 m, D_{50} ranges from 23 to 207 mm and D_{84} ranges from 62 to 558 mm. Bedload transport was measured with Helley-Smith samplers having 76.2-mm and 152.4-mm square orifices and a 0.25-mm mesh on the collecting bag. The bed surface diameters obtained by the pebble count method (applied with no truncation of the underrepresented fine end of the size distribution) were considered [*Wolman*, 1954]. Bedload transport was essentially composed of fine sediments whatever the slope, with a mean diameter approximately equal to 1 mm (Figure 2).

A second data set made up of 3,119 values was constructed with available data from the literature and is presented in Table 2. Both sand and gravel bed rivers were considered. Slopes at the study sites range from 0.0002 to 0.08, flow depths and widths associated with the discharges investigated range from 0.06 to 6.2 m and 0.3 to 170 m, respectively, D_{50} ranges

from 0.4 to 220 mm and D_{84} ranges from 0.9 to 543 mm. Only data including the flow discharge Q, the bedload transport rate Qs, the channel width W, the slope S, and the characteristic grain diameters D_{50} and D_{84} of the surface bed material were retained. Not all the available data sets of the literature were considered. For instance, *Bunte and Abt* [2005] measured bedload transport associated with diameters higher than 4 mm only, whereas measurements from *King et al.* [2004] indicated that for similar low flow conditions the median diameter of the transported material was essentially 1 mm (Figure 1). Consequently, their data were not used for the comparison. The Oak Creek data measured during the winter of 1969–1970 (data used for calibrating the vortex tube) were considered by *Milhous* [1973] to be poor quality and were not used. The slope estimate with a Strickler equation appeared uncertain in *Rankl and Smalley* [1992] and consequently, these data were not used.

For most field investigations, grain sizes were obtained from a graphical reading of the grain size curve. However, bed surface grain sizes were poorly described, in most cases with a single measurement for several years of investigation (for instance, for the Snake and Clearwater Rivers, a single curve is available for the year 1972, whereas bedload was measured over the period 1972–1979). In other cases, bed surface grain size was measured far away from the bedload measurement station (for instance, the Wind River grain surface was determined 1 mile downstream from the measurement station). When the surface bed material was sampled at different locations, the results were averaged to retain the characteristic grain surface diameters (Several of the Idaho rivers [*King et al.*, 2004], the Wind River, the Borgne d'Arolla River, several of the river data reported by *Williams and Rosgen* [1989]). More generally, in addition to the grain size measurement, all data sets are associated with several sources of uncertainty (measurement error, sampling efficiency, supply limitation) which will be considered in the discussion.

FIELD DATA ANALYSIS

Comparison with uniform sediment data

Which diameter should be used to characterize the armor layer? Bed surface diameters D_{50} and D_{84} will be considered because they are available in almost all published data sets. Both diameters could be used a priori as a descriptor of the armor layer mobility. Field bedload values from *King et al.* [2004] were plotted in Figure 3a after scaling both the Einstein parameter Φ and the Shields number θ (calculated with the measured hydraulic radius R) with the median grain size D_{50}. Flume data [*Recking et al.*, 2008b] are also plotted for comparison. The first observation is that most transport rates measured in the field are weaker than values investigated in flume experiments. One can deduce from this figure that the scatter is quite substantial, and that a single Shields number can be associated with bedload transport values covering almost seven orders of magnitude (θ=0.03 is associated with 1E−9< Φ < 1E−2). The same data were plotted in Figure 3b by replacing the measured hydraulic radius with the hydraulic radius calculated with Eq. 1. For the data set considered, the ratios between computed and measured values were in the range [0.6–1.2]. A first inspection of the figure indicates that the scatter is still wide and that other parameters should be considered. In the following, every time the hydraulic radius R is mentioned, it refers to values computed with the friction law. The field data set was plotted in Figure 3c with the Shields number θ and the Einstein parameter Φ calculated with D_{84} instead of D_{50}. One can observe that when using this method the field data broadly overlap with the flume data. However, the data remain widely scattered. In an attempt to reduce this scatter, the Shields number θ_{84} was scaled with a slope-dependent critical Shields stress $\theta_{c84}(S)$ calculated for the grain diameter D_{84} (using Eq. 4); the results are plotted in Figure 3d. Uniform sediment data and the formula derived for uniform sediment (Eq. 5) are also plotted for comparison. Scaling the Shields number with its critical

value did not really reduce the field data scatter, as was obtained with flume data. Let us consider a discrepancy ratio r defined as:

$$r = q_{s\,Computed} \Big/ q_{s\,Measured} \tag{6}$$

Only 18% of the r values fall within the range [0.1–10] when field data are compared with values calculated with the uniform sediment model (Eq. 5). The score is 15% when D_{50} is used instead of D_{84}. Such models derived for uniform sediments are undoubtedly unable to predict bedload transport in the field, especially at low Shields stress, when the characteristic grain size is chosen for the armor layer. In the following analyses, D_{84} will be used to characterize the armor layer and this parameter will be considered again in the discussion.

Hiding effects and formula derivation

The field data plotted in Figure 3d progressively deviate from the formulas derived for uniform sediment (Eq. 5). If we consider that the only difference between flume and field measurements is the sediment grain size gradation, one could logically assume that deviation from Eq. 5 should be consistent with the grain size gradation deviation from the uniform case. The choice of a grain sorting parameter is delicate. Using the data from *King et al.* [2004], *Pitlick et al.* [2008] observed that both the surface D_{50} and D_{84} vary with reach average shear stress, but not at the same rate: as channel gradient and shear stress increase toward the headwaters, the difference between D_{50} and D_{84} (and consequently hiding effects) increases. Thus, the D_{84}/D_{50} ratio could be a simple and useful way to take hiding effects into account, given that one objective of this paper is to derive a simple model, using available data only.

Figure 4 plots bedload data considering this ratio (only 20 Idaho rivers were considered for the sake of clarity) and indicates that the higher transport rates were associated with lower D_{84}/D_{50} ratios. Because bedload transport in these rivers essentially comprised fine sediments

(Figure 2), this result suggests that for a given flow condition (assumed to be controlled by D_{84}), the larger the D_{84}/D_{50} ratio was, (1) the greater the distance was between the main flow and the fine sediments deposited between large diameters making up the armor layer, (2) the higher the hiding effects were, and (3) the lower the transport rate was.

A bedload transport function was investigated in the form of a power law in an attempt to collapse the field data presented in Figure 4:

$$\Phi = \alpha\left(\frac{\theta_{84}}{\theta_{c84}}\right)^{\beta} \tag{7}$$

Coefficient β imposes the slope of the function and was fitted visually as 6.5 (Figure 4). Coefficients α vary with D_{84}/D_{50}. Once again, a power function was investigated and the coefficients used to draw the 5 curves in Figure 4 were fitted as a function of D_{84}/D_{50} on Figure 5a, producing a function of the form:

$$\alpha = 0.0005\left(\frac{D_{84}}{D_{50}}\right)^{-\gamma} \tag{8}$$

Whereas the value of γ was approximately 2 for all the data considered in Figure 4, it could not be applied to the entire *King et al.* [2004] data set, especially for very low and very steep slopes. This is why a second adjustment is proposed in Figure 5b, based on a few rivers of the data set including North Fork Clearwater (the flattest in the data set with S=0.0005) and Egger Creek (the steepest in the data set with S=0.07), leading to:

$$\gamma = 18S^{0.5} \tag{9}$$

This result suggests that for a given D_{84}/D_{50} ratio, the hiding effects increase with increasing slope (and that consequently the rates are decreased for a given θ/θ_c ratio). Such a slope effect is hard to explain (it is likely closely linked to the flow turbulence properties on steep slopes,

which are still poorly known). Finally, the entire data set was fitted with the following function:

$$\Phi = 0.0005\left(\frac{D_{84}}{D_{50}}\right)^{-18\sqrt{S}}\left(\frac{\theta_{84}}{\theta_{c84}}\right)^{6.5} \quad (10)$$

This equation permits reproduction of the 3,200 field data from *King et al.* [2004], with 83% of the calculated values verifying [$0.1 < r < 10$]. It can be compared with the uniform sediment bedload equation by replacing θ/θ_c in Eq. 5 by the following function:

$$\frac{\theta}{\theta_c} = 1.2\left(\frac{D_{84}}{D_{50}}\right)^{-1.4\sqrt{S}}\sqrt{\frac{\theta_{84}}{\theta_{c84}}} \quad (11)$$

This correction, used for comparison with transport of uniform sediments, considers that the grain shear stress associated with the flow holds for the bed surface D_{84} and corrects this shear stress for transport of finer sediments through a hiding effect calculated as a function of the slope and the distance measured between D_{84} and D_{50}. It allows us to collapse the Idaho bedload data with the uniform sediment model (Eq. 5) in Figure 6a.

Bedload transport equation

Equation 10 was derived from the *King et al.* [2004] data set, and Figure 3 suggests that it would be representative for low flow conditions only (phase 1 of transport). A full model should be able to represent all transport phases. Intense bedload transport is difficult to measure in the field. It is usually associated with almost equal mobility for all particle sizes present [*Parker and Klingeman*, 1982]. This was demonstrated in flume experiments [*Recking et al.*, 2009], where transport of poorly sorted sediments corresponded to almost equal mobility every time $\theta/\theta_c > 2$ approximately. With uniform sediments [*Recking et al.*, 2008b], this threshold also corresponded to the transition between the two parts of the model (Eq. 5). Whereas the first member of Eq. 5 was characterized by partly mobile grains moving in a

discontinuous bedload layer, the second member was associated with fully mobile grains transported in a continuous and uniform bedload layer [*Recking et al.*, 2008a]. In both cases (uniform and poorly sorted sediments), what seems to characterize intense transport is full mobility of the grains, with no sorting effects. This is why, as a first approximation, the model derived for intense transport of uniform sediments (second member of Eq. 5) will be used for modeling the gravel-bed transport in phase 3. Once again, and as an extension to what was observed for flow resistance, D_{84} will be considered for comparison with uniform sediments. However, the turbulence properties of such flows are still poorly known and this hypothesis needs to be validated by comparisons with measurements. In addition, none of the *King et al.* [2004] field data correspond to the transition between low and intense transport and at this stage of the study, the use of Eq. 10 will be extended to higher flow conditions. The final equation is:

$$\Phi = 0.0005\left(\frac{D_{84}}{D_{50}}\right)^{-18\sqrt{S}}\left(\frac{\theta_{84}}{\theta_{c84}}\right)^{6.5} \quad \text{for } \theta_{84}/\theta_{c84} < \mathrm{L}$$
$$\Phi = 14\theta_{84}^{2.45} \quad \text{for } \theta_{84}/\theta_{c84} > \mathrm{L} \tag{12}$$

θ_{c84} being calculated with Eq. 4. The breakpoint L between the two parts of the model should be rigorously calculated by an iterative approach (for equaling both parts of Eq. 12) for each (S, D_{84}/D_{50}) value. It can also be approximated by the following function:

$$L = 33\left(\frac{D_{84}}{D_{50}}\right)^{0.85} S + 2\left(\frac{D_{84}}{D_{50}}\right)^{-0.7} \tag{13}$$

Finally, bedload transport is given by:

$$q_s[kg/s/m] = \rho_s\sqrt{g(s-1)D_{84}^3}\,\Phi \tag{14}$$

with $\rho_s \approx 2650$ kg/m^3 for natural sediments.

MODEL CONFIRMATION

Equation 12 was tested in comparison with formulas from *Meyer-Peter and Mueller* [1948], *Parker* [1979], and *Schoklitsch* [1962] (all presented in the appendix). The Meyer-Peter Mueller and the Parker equations were chosen because they permit a surface-based calculation with limited knowledge of sediment characteristics and they are widely used. These two equations include a constant critical Shields stress (0.047 and 0.03, respectively). The *Schoklitsch* [1962] equation was interesting to compare because it provides a direct calculation of the bedload transport rate from the flow discharge, without calculating shear stress, and has been found to apply well to flume data for slopes in the range of $0.0025 < S < 0.2$ [*Bathurst et al.*, 1987]. However, this equation is used here with the bed surface D_{50} as a characteristic diameter (as often done), whereas considering the original work, the formula was actually derived for the D_{40} of the subsurface material [*Bathurst*, 2007].

Equation 12 was tested first on data from the Idaho rivers (see auxiliary material). The correlation between measured and calculated values was good when considering each river individually. This is illustrated with the river selection plotted in Figure 7. In all cases, the data plotted within the range $[0.1<r = qs_{calculated}/qs_{measured}<10]$ and parallel (just above or just below) to the line of perfect equality. The results presented in Table 3 indicate the score obtained by the models for each of the data set's 33 rivers. Contrary to previous approaches, the method presented in this paper gave a very satisfactory result with 83% of the values verifying $[0.1< qs_{calculated}/qs_{measured}<10]$.

Of course, this was not a pertinent test for Eq. 12 because this data set was used to fit the equation. A second test was performed with the data presented in Table 2 (see auxiliary material). The correction with Eq. 11 allows us to collapse these data with the uniform

sediment model (Eq. 5) in Figure 6b. The results presented in Table 4 indicate that Eq. 12 has a score of 86%, which can be considered a very good result for a blind test.

Formulas were tested within one order of magnitude ($0.1 < r < 10$), because for all the data sets considered, this interval of precision was associated with bedload measurements for a given flow discharge. It corresponds to the fluctuations that naturally exist in the transport of poorly sorted sediments (because of grain sorting), appropriately reproduced in flume experiments even with perfectly controlled and constant water and sediment feed [*Iseya and Ikeda*, 1987; *Kuhnle and Southard*, 1988; *Recking et al.*, 2009]. The discrepancy ratio interval was reduced in Table 5. The results indicate that the model's performance is still good when considering smaller-range values for r and that Eq. 12 does better than the alternatives whichever value of r is preferred.

Calculated and measured values are plotted in Figure 8 for each model. The points plotted parallel to the y-axes for $q_{scal}=10E^{-4}$ correspond to data where formulas predicted a zero transport, whereas the measurement was not zero. The Parker equation result is consistent with Figure 4, with an overestimation for high rates and underestimation for low rates. This may be because this equation was partly calibrated with flume data. Figure 8 indicates that formulas including a threshold value for transport did not reproduce the low transport rate data well. More particularly, the *Meyer-Peter and Mueller* [1948] formula could not reproduce the data from *King et al.* [2004] at all, which nearly all correspond to transport phase 1. This is why formula efficiency was tested taking the transport phases into account. Since there is not yet a clear definition for the transition between phases, three transport phases are defined hereafter, considering D_{84} mobility and flume experiment observations [*Recking et al.*, 2008a; *Recking et al.*, 2009]:

- Phase 1 ($\theta_{84}/\theta_{c84}<1$): D_{84} is immobile, but part of the surface diameters smaller than D_{84} are assumed to be destabilized and/or transported.
- Phase 2 ($1<\theta_{84}/\theta_{c84}<2$ approximately): once D_{84} is destabilized, all the surface grain diameters are assumed to be destabilized and/or partially mobile.
- Phase 3 ($2 < \theta_{84}/\theta_{c84}$): the armor layer is fully mobile.

The θ_{84}/θ_{c84} limit equals 2 corresponds to a mean value given by Eq. 13 and was observed to be a good threshold value for near equal mobility in the transport of poorly sorted sediments by *Recking et al.* [2009]. The data set presented in Table 2 is valuable because it includes all phases of transport (1,754 values in phase 1, 769 values in phase 2, and 596 values in phase 3) and was used to test the efficiency of each formula (by calculating for each run the discrepancy ratio r) with respect to each phase (note that the values selected for phase 3 with the previous criteria also satisfied the condition $\theta_{84}/\theta_{c84}>L$ in Eq. 12). Results presented in Table 6 confirm that the model, developed from phase 1 data [*King et al.*, 2004] and flume data, is valid whatever the sediment transport intensity. This is illustrated with Figure 9 where a comparison between calculated and measured values for several rivers is plotted. Table 6 also indicates that the usual surface-based formula (derived from flume experiments with near uniform sediments) is only valid in phase 3, i.e., when the larger surface grain diameters are in motion. In field applications, such intense bedload transport corresponds to large floods, whereas the bedload transport rates of phases 1 and 2 are associated with near bankfull discharge [*Ryan et al.*, 2002], i.e., common floods responsible for the long-term channel morphology changes.

DISCUSSION

Domain validity

Because bedload fluctuations naturally exist for a given flow discharge, Eq. 12 will at best give the mean bedload transport value. This is why the mean values of the ratio $r = qs_{calculated}/qs_{measured}$ were plotted in Figure 10. This figure suggests that Eq. 12 is valid in the range $0.0002 < S < 0.08$ and $0.9 < D_{84}(\text{mm}) < 558$. Sand river data (Chippewa River, Wisconsin River, Yampa River, Black River, Muddy Creek) were measured in phase 3 of transport and were consequently tested on the second member of Eq. 12 only. Actually, testing the first member of this equation on sand river bedload transport would require considering very low transport rates associated with low flow conditions (flow depth lower than approximately 20 cm for a 0.0002 slope), which are not within the scope of most field applications. The second member of Eq. 12 was also validated for slopes up to 20% with flume data in *Recking et al.* [2008b]. Extending this result to field applications would require defining an appropriate flow resistance equation for steep slopes [*Rickenmann*, 1994; *Ferguson*, 2007].

Supply limitation

Equation 12 was developed by considering implicitly that fine sediments are always available for transport, whatever the flow intensity. However, this may not always be true. The effect of sand content in the transported material was rigorously tested in recirculated flume experiments by *Wilcock et al.* [2001], and their data (runs BMC, J27, J21, J14 and J06) were used to test Eq. 12. Results of the comparison between calculated and measured values are plotted in Figure 11a (the algorithm presented in *Recking* [2006] takes into account the flume side wall effect). Figure 11b plots the mean value of ratio $r = qs_{calculated}/qs_{measured}$ obtained in each run, as a function of the proportion of sand at the bed surface F_s reported in Wilcock et

al. [2001] (their Figure 3). Flume results indicate that the model efficiency is good ($r \approx 1$) when sand is present at the bed surface and decreases when the percentage of sand is decreased. This limitation was not as severe in the field, given that several of the data sets from *King et al.* [2004] were well predicted despite the surface grain size distribution indicated as less than 5% sand. New field measurements would be necessary to investigate this point. However, it would essentially concern low transport (lower than 1 g/s/m), which may be negligible in many field applications.

Characteristic grain size

Diameter D_{84} was used as a characteristic grain size of the bed pavement in this study instead of D_{50}. However, similar work (not presented here) was carried out by fitting the *King et al.* [2004] data with θ_{50}/θ_{c50} instead of θ_{84}/θ_{c84} (but still using D_{84} in the flow resistance equation). It produced an equation similar to Eq. 12 (except for the coefficient affecting the D_{84}/D_{50} exponent, which was 10 instead of 18) with the same performance when compared to the results presented in Table 6 (87% for phase 1 data and 76% for phase 2 data). In fact, selecting the appropriate characteristic grain size is problematic when equations derived for uniform sediments (i.e., the second member in Eq. 5) are used in the field (i.e., the second member in Eq.12). The 89% score presented in Table 6 for phase 3 data drops to 73% when θ_{50} is used instead of θ_{84}, suggesting that D_{84} is more appropriate. Additional measurements (in the flume or in the field) are needed before a conclusion on this question can be drawn.

Model sensitivity to the grain size measurement

The bed surface diameters are associated with large uncertainties: (1) for most of the data sets used, the bed surface grain sizes were poorly described, with in most cases a single measurement for several years of investigation, (2) different measurement techniques were

used (Table 2) and (3) the model implicitly assumes that the surface texture measured at low flow is valid during flooding. *Clayton and Pitlick* [2008] showed that the third condition should be verified, at least when the availability of the various grain sizes in the supply is sufficient. Despite these uncertainties, relatively good scores were obtained with the diameters given by the authors (Table 3, Table 4), whatever method is used (sieving analyses or the pebble count method applied with no truncation of the underrepresented fine end of the size distribution). Actually, additional computations (not presented here) indicated that the 86% score shown in Table 4 was still good (above 80%) when the median diameter D_{50} of the whole data set (Table 2) was varied within 30%. In some cases (for instance Goodwin Creek) this score was even improved. Thus, if errors made in grain size measurements are not too large, bedload prediction errors with Eq. 12 should be reasonable. Conversely, large uncertainties in grain size measurement strongly impact bedload prediction, as illustrated with Clearwater [*Seitz*, 1976] and North Fork Clearwater [*King et al.*, 2004]. The Clearwater River grain size distribution was measured by sieve analysis and the pebble count method (truncated at 4 mm), producing D_{84}/D_{50} values equal to 3.5 and 1.8, respectively. Two curves were also defined for the North Fork Clearwater River with the nontruncated pebble count technique between 1994 and 1995, producing D_{84}/D_{50} values equal to 4.5 and 2. These very different grain size distributions led to totally different results when used in the computation (Figure 12).

Relevance of data used for the model construction and validation

The model's accuracy also depends on the quality of data used for its calibration. The Helley-Smith sampler efficiency has been investigated in many studies [*Emmett*, 1980; *Hubbell and Stevens*, 1986; *Childers*, 1999; *Ryan and Porth*, 1999; *Sterling and Church*, 2002; *Bunte and Abt*, 2005; *Ryan et al.*, 2005; *Vericat et al.*, 2006] and the results are very contradictory.

Because of the small size of the H-S orifice, the catch efficiency is particularly questionable for high transport rates, with large pebbles moving only at this time, likely resulting in underestimation. The bedload equation (Eq. 12) was fitted on low transport rate data, for which orifice size (76 mm) was much larger than the collected material for most of the river reaches investigated (Figure 2), minimizing the risk of a bias. Overall, this study did not bring out fundamental differences in the results obtained when the model was tested on data sets collected with the standard Helley-Smith samplers (76.2 mm square entrance) and other techniques (Ebro River, Dupuyer Creek, Elbow River, Oak Creek, East Fork, flume experiments).

Other sources of uncertainties

In addition to the main limitations mentioned earlier, many other sources of uncertainty could explain the differences between the measured and computed values:

(i) The flow hydraulic measurements (especially when there is no gauging station).

(ii) Estimate of the active width used for applying one-dimensional bedload transport formulas to field situations that are fully two-dimensional [*Ferguson*, 2003].

(iii) The slope value (usually only one bed slope value is available for a measurement period over several years, whereas the energy slope should be rigorously used for each event).

CONCLUSION

The objective of this study was to investigate further the ability of simple equations to predict mean bedload transport, with limited knowledge of the bed surface material, i.e., diameters D_{50} and D_{84}. The analyses were based on the Idaho river data produced by *King et al.* [2004] as well as on recently published results on bedload and flow resistance modeling [*Recking et al.*, 2008b] and critical Shields stress [*Recking*, 2009].

The Idaho field data were first compared with a data set comprising 1,317 values obtained with uniform sediments in flume experiments [*Recking et al.*, 2008b]. The conclusion was that no comparison is possible between the field and the flume data, whatever the diameter – D_{50} or D_{84} – used for scaling the field data. One reason for this is that most of the field transport rates considered were much lower than values investigated in the flume experiments. Consequently, extending a uniform sediment transport model to field application was not straightforward, and a new model was fitted on the field data. This model expressed as a function of the ratio between the Shields stress and its threshold value for transport (θ/θ_c) incorporated a very simple hiding function depending on the bed surface D_{84}/D_{50} ratio and the slope. Because the field data from *King et al.* [2004] corresponded to low transport rates only, the uniform sediment model was used to extend its applicability to intense bedload transport. This required choosing a characteristic grain size and D_{84} appeared to be more appropriate.

Bedload calculation with the approach proposed in this paper finally requires five entrance parameters (the flow discharge Q, the slope S, the surface grain diameter D_{50} and D_{84}, and the active width W) and three steps: shear stress calculation using the flow resistance equation (Eq. 1), the critical shear stress calculation for diameter D_{84} (Eq.4) and the bedload calculation (Eq. 12).

The model was compared with an independent data set of the literature made up of 3,119 field values, for which surface diameters D_{50} and D_{84} were poorly defined (usually only one measurement is available for several years of bedload measurement). However, despite these uncertainties, the formula proved to reproduce almost all the field data well, with precision within one order of magnitude and, unlike other equations, reproduced the data trend adequately.

The model was compared with common surface-based formulas considering three phases of transport [*Jackson and Beschta*, 1982; *Ashworth and Ferguson*, 1989; *Bathurst*, 2007], defined as follows: phase 1 (θ_{84}/θ_{c84} <1), where the diameter D_{84} is immobile and bedload transport is made up essentially of fine sediments (from upstream, patches of fine sediments, or the subsurface when smaller diameters of the armor layer are destabilized); phase 2 ($1<\theta_{84}/\theta_{c84}$ <2 approximately) for which all the surface grain diameters are partially mobile, with alternating zones of rest and mobility; and phase 3 ($2 < \theta_{84}/\theta_{c84}$) for which the armor layer is fully mobile. The new formula reproduced all the transport phases particularly well, and above all, the low bedload transport rates associated with phases 1 and 2. The usual surface-based formulas gave satisfactory results only for phase 3 and showed a very poor performance for phases 1 and 2. However, the low transport rates in phases 1 and 2 correspond to near bankfull discharge in most rivers and cannot be insignificant in a river sediment budget or for estimating the long-term morphological changes [*Barry et al.*, 2008].

If this model is confirmed with new field experiments, it will be valuable for field applications because it is not time- and data-consuming (as is the case for fractional-based calculations) and, since it does not need calibration, it provides a rapid estimate of the bulk transport rate. However, several aspects need to be considered in further research including the effects of

supply limitation (more particularly for the sand fraction), the model's sensitivity to the grain surface measurement procedure, and the appropriate characteristic grain diameter for intense transport.

APPENDIX

a) The *Meyer-Peter and Mueller* [1948] equation is:

$$q_s[kg/s/m] = 8\rho_s\sqrt{g(s-1)D_{50}^3}\left(\left(\frac{n'}{n}\right)^{3/2}\theta - 0.047\right)^{3/2} \quad (15)$$

with ρ_s=2650 kg.m^{-3}, ρ=1000 kg.m^{-3} and s=2.65. The n'/n ratio used in the *Meyer-Peter and Mueller* [1948] equation is the ratio of particle roughness n' to total roughness n, which corrects the total boundary shear stress to the skin friction stress. The n term is estimated with the equation (n=$S^{1/2}R^{2/3}/U$) and n′ is calculated with the *Strickler* [1923] equation (n'=$D_{90}^{1/6}$/26).

b) The *Parker* [1979] equation is:

$$q_s[kg/s/m] = 11.2\rho_s\sqrt{g(s-1)D_{50}^3}\,\frac{(\theta-0.03)^{4.5}}{\theta^3} \quad (16)$$

It was used with the following flow resistance equation to determine R associated with the bed resistance [*Hey*, 1979]:

$$\frac{U}{\sqrt{gRS}} = 6.25 + 5.75\log\left(\frac{R}{3.5D_{84}}\right) \quad (17)$$

This equation was shown to be a good approximation of Eq.1 in *Recking et al.* [2008b].

c) The *Schoklitsch* [1962] equation is:

$$q_s[kg/s/m] = 2.5S^{1.5}\rho(q-q_c) \quad (18)$$

where q is the water discharge per unit width (m^{3}s^{-1}m^{-1})

$$q_c = 0.0612g^{0.5}D_{40}^{1.5}S^{-1.17} \quad (19)$$

ACKNOWLEDGMENTS

This study was supported by the Cemagref, the PGRN (Pole Grenoblois des Risques Naturels), and the ANR GESTRANS project.

This study would not have been possible without the USDA and the USGS data sets, as well as all the other published data sets presented in Table 2.

The author would like to thank Rob Ferguson, John Pitlick, and other anonymous reviewers who greatly contributed to this paper by providing helpful reviews of an earlier version of this manuscript. Thanks are extended to Gordon Grant (Associate Editor), who contributed to this paper by providing additional reviews.

REFERENCES

Almedeij, J. H. (2002), Bedload Transport in gravel-bed streams under a wide range of Shields stresses, 111 pp, Blacksburg, Virginia.

Almedeij, J. H., and P. Diplas (2003), Bedload transport in gravel-bed streams with unimodal sediment, *Journal of Hydraulic Engineering (ASCE)*, *129*, 896-904.

Andrews, E. D. (1994), Marginal bed load transport in a gravel bed stream, Sagehen Creek, California, *Water Resources Research*, *30*, 2241-2250.

Andrews, E. D. (2000), Bed material transport in the Virgin River, Utah, *Water Resources Research*, *36*, 585.

Ashworth, P. J., and R. Ferguson (1989), Size-selective entrainment of bed load in gravel bed streams, *Water Resources Research*, *25*, 627-634.

Barry, J. J., J. M. Buffington, P. Goodwin, J. G. King, and W. W. Emmett (2008), Performance of bedload transport equations relative to geomorphic significance: predicting discharge and its transport rate, *Journal of Hydraulic Engineering (ASCE)*, *134*, 601-615.

Barry, J. J., J. M. Buffington, and J. G. King (2004), A general power equation for predicting bed load transport rates in gravel bed rivers, *Water Resources Research*, *40*, 1-22.

Batalla, R. J. (1997), Evaluating bed material transport equations using field measurements in a sandy gravel-bed stream, Arbucies, NE Spain, *Earth Surface Processes and Landforms*, *22*, 121-130.

Bathurst, J. C. (2007), Effect of coarse surface layer on bed-load transport, *Journal of Hydraulic Engineering (ASCE)*, *133*, 1192-1205.

Bathurst, J. C., W. H. Graf, and H. H. Cao (1987), Bed load discharge equations for steep mountain rivers, in *Sediment Transport in Gravel Bed Rivers*, edited by C.R.Thorne, J.C.Bathurst and R.D.Hey, pp. 453-491, John Wiley & Sons Ltd.

Bravo-Espinosa, M., W. R. Osterkamp, and V. L. Lopes (2003), Bedload transport in alluvial channels, *Journal of Hydraulic Engineering (ASCE)*, *129*, 783-795.

Bunte, K., and S. R. Abt (2005), Effect of sampling time on measured gravel bed load transport rates in a coarse-bedded stream, *Water Resources Research*, *41*, 12 pp.

Cardoso, A. H., and G. O. Neves (1994), Prévision du transport solide total : Evaluation de formules existantes, *Houille Blanche*, *4*, 13-22.

Childers, D. (1999), Field Comparisons of six pressure-difference bedload samplers in high-energy flow, USGS report N°92-4068, 59 pp

Clayton, A., and J. Pitlick (2008), persistence of the surface texture of a gravel-bed river during a large flood, *Earth Surface Processes and Landforms*, *33*, 661-673, doi: 10.1002/esp.1567.

Egiazaroff, I. V. (1965), Calculation of nonuniform sediment concentrations, *Journal of the Hydraulics Division (ASCE)*, *HY4*, 225-247.

Einstein, H. A. (1950), The bed-load function for sediment transportation in open channel flows, Technical Bulletin N°1026, United States Department of Agriculture - Soil Conservation Service, Washington, 71 pp

Einstein, H. A., and N. Chien (1953), Transport of sediment mixtures with large ranges of grain sizes, UniV. of Calif. Inst. of Eng., 49 pp

Emmett, W. W. (1980), A field calibration of the sediment-trapping characteristics of the Helley-Smith bedload sampler, USGS Report N°1139, 44 pp

Emmett, W. W., R. M. Myrick, and R. H. Meade (1980), Field data describing the movement and storage of sediment in the East Fork River, Wyoming. part 1: River Hydraulics and Sediment Transport, 1979, Denver, Colorado, USGS Report N°80-1189, 43 pp

Emmett, W. W., and H. R. Seitz (1974), Suspended - and bedload- sediment transport in the Snake and Clearwater rivers in the vicinity of Lewiston, Idaho (July 1973 through July 1974), Boise, Idaho, U. R. S. a. b. D. report),

Ferguson, R. (2007), Flow resistance equations for gravel and boulder bed streams, *Water Resources Research*, *43*, 1-12.

Ferguson, R. I. (2003), The missing dimension: effects of lateral variation on 1-D calculations of fluvial bedload transport, *Geomorphology*, *56*, 1-14.

Gomez, B. (1988), Two data sets describing channel-wide temporal variations in bedload-transport rates, Colorado, U. R. N. 88-88, 26 pp

Gomez, B., and M. Church (1989), An assessment of bedload sediment transport formulae for gravel bed rivers, *Water Resources Research*, *25*, 1161-1186.

Hey, R. D. (1979), Flow resistance in gravel bed rivers, *Journal of the Hydraulics Division (ASCE)*, *105*, 365-379.

Hollingshead, A. B. (1971), Sediment transport measurement in gravel river, *Journal of the Hydraulics Division (ASCE)*, *HY11*, 1817-1834.

Hubbell, D. W., and H. H. Stevens (1986), Factors affecting accuracy of bedload sampling, paper presented at Proc, 4th Federal Interagency Sedimentation Conf., Subcomm. on Sedimentation, Interagency Advisory Commitee on Water Data, Las Vegas.

Iseya, F., and H. Ikeda (1987), Pulsations in bedload transport rates induced by a longitudinal sediment sorting: a flume study using sand and gravel mixture, *Geografiska Annaler*, *69A*, 15-27.

Jackson, W. L., and R. L. Beschta (1982), A model of two-phase bedload transport in an Oregon coast range stream, *Earth Surface Processes and Landforms*, *7*, 517-527.

Jones, M. L., and H. R. Seitz (1980), Sediment transport in the Snake and Clearwater rivers in the vicinity of Lewiston, Idaho, U. r. 80-690, 179 pp

King, J. G., W. W. Emmett, P. Whiting, S. T. Kenworthy, and J. J. Barry (2004), Sediment transport data and related information for selected corse-bed streams and rivers in Idaho, USDA, (http://www.fs.fed.us/rm/boise/research/watershed/BAT/)

Kuhnle, R. A. (1992), Fractional transport rates of bedload on Goodwin Creek, in *Dynamics of gravel bed rivers*, edited by P.Billi, R. D. Hey, C. Thorne and P. Tacconi, pp. 141-155, John Wiley & Sons.

Kuhnle, R. A., and J. B. Southard (1988), Bed load transport fluctuations in a gravel bed laboratory channel, *Water Resources Research*, *24(2)*, 247-260.

Lamb, M. P., W. E. Dietrich, and J.-G. venditti (2008), Is the critical Shields stress for incipient sediment motion dependent on channel-bed slope?, *J. Geophys. Res.*, *113*.

Leopold, L. B., and W. W. Emmett (1976), Bedload measurements, East Fork River, Wyoming, *Proc. Nat. Acad. Sct. USA*, *73*, 1000-1004.

Leopold, L. B., and W. W. Emmett (1977), 1976 Bedload measurements, East Fork River, Wyoming, *Proc. Nat. Acad. Sct. USA*, *73*, 2644 - 2648.

Leopold, L. B., and W. W. Emmett (1997), Bedload dand River Hydraulics - Inferences from the East Fork River, Wyoming, USGS Professional Paper 1583, 52 pp

Lisle, T. E. (1986), Stabilization of a gravel channel by large streamside obstruction and bedrock bends, Jacoby Creek, Northwestern California, *Geological Society of America Bulletin*, *97*, 999-1011.

Lisle, T. E. (1989), Sediment transport and resulting deposition in Spawning Gravels, North Coastal California, *Water Resources Research*, *25*, 1303-1319.

Martin, Y. (2003), Evaluation of bedload transport formulae using fields evidence from the Vedder River, British Colombia, *Geomorphology*, *53*, 73-95.

Meyer-Peter, E., and R. Mueller (1948), Formulas for Bed-Load Transport, paper presented at Procedings 2d Meeting IAHR, Stockholm.

Milhous, R. T. (1973), Sediment transport in a gravel-bottomed stream, Oreg. State Univ., Corvallis.

Molinas, A., and B. Wu (1998), Effect of size gradation on transport of sediment mixtures, *Journal of Hydraulic Engineering (ASCE)*, *124*, 786-793.

Mueller, E. R., J. Pitlick, and J. M. Nelson (2005), Variation in the reference Shields stress for bed load transport in gravel-bed streams and rivers, *Water Resources Research*, *41*, W04006 (04001-04010).

Muskatirovic, J. (2008), Analysis of bedload transport characteristics of Idaho streams and rivers, *Earth Surface Processes and Landforms*, *33*, 1757-1768, doi:10.1002/esp^.1646.

Parker, G. (1979), Hydraulic geometry of active gravel rivers, *Journal of Hydraulic Engineering (ASCE)*, *105*, 1185-1201.

Parker, G. (1990), Surface-based bedload transport relation for gravel rivers, *Journal of Hydraulic Research*, *28*, 417-428.

Parker, G., and P. C. Klingeman (1982), On why gravel bed streams are paved, *Water Resources Research*, *18*, 1409-1423.

Parker, G., P. C. Klingeman, and D. G. McLean (1982), Bedload and size distribution in paved gravel-bed streams, *Journal of the Hydraulics Division (ASCE)*, *108*, 544-571.

Pitlick, J., E. R. Mueller, C. Segura, R. Cress, and M. Torizzo (2008), Relation between flow, surface layer armoring and sediment transport in gravel bed rivers, *Earth Surface Processes and Landforms*, *DOI:10.1002/esp.1607*, 18.

Rankl, J. G., and M. L. Smalley (1992), Transport of sediments by streams in the Sierra Madre, Southern Wyoming, USGS report N° 92-4091,

Recking, A. (2006), An Experimental Study of Grain Sorting Effects on Bedload, 261 pp, PhD Thesis Cemagref (http://cemadoc.cemagref.fr/), Lyon.

Recking, A. (2009), Theoretical development on the effects of changing flow hydraulics on incipient bedload motion, *Water Resources Research*, *45, W04401*, 16, doi:10.1029/2008WR006826.

Recking, A., P. Frey, A. Paquier, and P. Belleudy (2009), An experimental investigation of mechanisms responsible for bedload sheet production and migration, *J. Geophys. Res.*, *114*doi:10.1029/2008JF000990.

Recking, A., P. Frey, A. Paquier, P. Belleudy, and J. Y. Champagne (2008a), Bedload transport flume experiments on steep slopes, *Journal of Hydraulic Engineering*, *134*, 1302-1310, DOI:10.1061/(ASCE)0733-9429(2008)134:9(1302).

Recking, A., P. Frey, A. Paquier, P. Belleudy, and J. Y. Champagne (2008b), Feedback between bed load and flow resistance in gravel and cobble bed rivers, *Water Resources Research*, *44*, 21, doi:10.1029/2007WR006219.

Reid, I., J. B. Laronne, and D. M. Powell (1995), The Nahal Yatir Bedload database: sediment dynamics in a gravel-bed ephemeral stream, *Earth Surface Processes and Landforms*, *20*, 845-857.

Rickenmann, D. (1991), Hyperconcentrated flow and sediment transport at steep slopes, *Journal of Hydraulic Engineering (ASCE)*, *117*, 1419-1439.

Rickenmann, D. (1994), An alternative equation for the mean velocity in gravel-bed rivers and mountain torrents, paper presented at Hydraulic Engineering, Buffalo.

Ryan, S., and L. Porth (1999), A field comparison of three pressure-difference bedload samplers, *Geomorphology*, *30*, 307-322.

Ryan, S., L. Porth, and C. Troendle (2005), Coarse sediment transport in mountain streams in Colorado and Wyoming, USA., *Earth Surface Processes and Landforms*, *30*, 269-288.

Ryan, S. E., L. S. Porth, and C. A. Troendle (2002), Defining phases of bedload transport using piecewise regression, *Earth Surface Processes and Landforms*, *27*, 971-990.

Schoklitsch, A. (1962), *Handbuch des Wasserbaus (in German), Springer Verlag (3rd edition)*, Wien.

Seitz, H. R. (1976), Suspended - and bedload- sediment transport in the Snake and Clearwater rivers in the vicinity of Lewiston, Idaho (August 1975 through July 1976), Boise, Idaho, U. R. F. a. b. D. report),

Smalley, M. L., W. W. Emmett, and A. M. Wacker (1994), Annual eeplenishment of bed material by sediment transport in the Wind River near Riverton, Wyoming, Cheyenne, U. R. 94-4007,

Sterling, M. S., and M. Church (2002), Sediment trapping characteristics of a pit trap and the Helley-Smith sampler in a cobble gravel bed river, *Water Resour. Res.*, *38*, 1-19.

Strickler, K. (1923), Beiträge zur Frage der Geschwindigkeitsformel und der Rauhigkeitszahlen für Ström, Kanäle und geschlossene Leitungen, paper presented at Eidgenössisches Amt für Wasserwirtschaft, Bern, Switzerland.

Vericat, D., M. Church, and R. J. Batalla (2006), Bedload bias: comparison of measurements obtained using two (76 and 152 mm) helley-Smith samplers in a gravel bed river, *Water Resour. Res.*, *42*, 1-13.

Whitaker, A. C., and D. F. Potts (2007), Analysis of flow competence in an alluvial gravel bed stream, Dupuyer Creek, Montana, *Water Resources Research*, *43*, 1-16.

Wilcock, P. R., and J. C. Crowe (2003), Surface-based transport model for mixed-size sediment, *Journal of Hydraulic Engineering (ASCE)*, *129*, 120-128.

Wilcock, P. R., and S. T. Kenworthy (2002), A two-fraction model for the transport of sand/gravel mixtures, *Water Resources Research*, *38*.

Wilcock, P. R., S. T. Kenworthy, and J. C. Crowe (2001), Experimental study of the transport of mixed sand and gravel, *Water Resources Research*, *37*, 3349.

Wilcock, P. R., and B. W. McArdell (1993), Surface-based fractional transport rates: Mobilization thresholds and partial transport of a sand-gravel sediment, *Water Resources Research*, *29*, 1297-1312.

Williams, G. P., and D. L. Rosgen (1989), Measured total sediment loads (suspended loads and bedloads) for 93 United States streams, USGS Open-File Report 89-67, 128 pp

Wolman, M. G. (1954), Method of sampling coarse river bed material, *Transactions of the American Geophysical Union,*, *35*, 951-956.

Yang, C. T., and C. Huang (2001), Applicability of sediment transport formulas, *Int. J. sediment research*, *16*, 335-353.

FIGURE CAPTIONS

Figure 1: Plot of the uniform sediment bedload transport rate values (a) versus the Shields number and (b) versus the ratio between the Shields number and its critical value

Figure 2: Median diameter of the transported material as a function of the slope (King et al. [2004] data)

Figure 3: Plot of the flume and field bedload transport data from King et al. [2004] versus the Shields number (a) with R measured and $D= D_{50}$; (b) with R calculated and $D= D_{50}$; (c) with $D=D_{84}$ as characteristic diameter; (d) with θ_{84} scaled with $\theta_c=\theta_c(S, D_{84})$. The line drawn on each figure represents the envelope of the hidden data.

Figure 4: Plot of field bedload transport as a function of θ_{84}/θ_{c84} considering the D_{84}/D_{50} ratio

Figure 5: a) Fit of coefficient α as a function of the ratio D_{84}/D_{50} and b) fit of coefficient γ as a function of the slope

Figure 6: Comparison between flume and field data after shear stress correction for hiding effects with Eq. 11 (a) King et al data and (b) data from Table 2 Table 2 (only data verifying $\theta_{84}/\theta_{c84} <$ L were plotted)

Figure 7: Comparison between calculated and measured bedload transport for several river reaches. Lines parallel to the line of perfect equality correspond to the range [$0.1<r = qs_{calculated}/qs_{measured}<10$]

Figure 8: Comparison between calculated and measured bedload transport for the entire field data sets (6,319 values). Values plotted parallel to the y-axis correspond to zero predictions

for nonzero measured bedload transport. Lines parallel to the line of perfect equality correspond to the range [$0.1<r = qs_{calculated}/qs_{measured}<10$]

Figure 9: Comparison between calculated and measured bedload transport for several rivers, considering each phase of transport. Lines parallel to the line of perfect equality correspond to the range [$0.1<r = qs_{calculated}/qs_{measured}<10$]

Figure 10: Plot of the ratio $r = qs_{calculated}/qs_{measured}$ as a function of the slope S and grain diameter D_{84}. Vertical lines are the standard error

Figure 11: a) Comparison between calculated and measured bedload transport using flume data [*Wilcock et al.*, 2001]; b) mean ratio $r = qs_{calculated}/qs_{measured}$ as a function of the percentage of sand on the bed surface

Figure 12: Model sensitivity to the sediment grain size for Clearwater River

TABLES

Parameter	Range
Slope (m/m)	0.001–0.2
Diameter (mm)	0.3–44.3
Shields number θ	0.014–3.43
Einstein parameter Φ	3.8E−9 – 264

Table 1: Main characteristics of flume data

Site	Data source	Measurement technique*
Oak Creek	*Milhous* [1973]	Sediment trap, vortex tube / GS / not specified
Sagehen	*Andrews* [1994]	HS (15 cm) / GS / not specified
Goodwin Creek	*Kuhnle* [1992]	HS (58 cm² with trapezoidal shape), 0.25mm net mesh / GS, energy slope measured / Sieving
Nahal Yatir	*Reid et al.* [1995]	Sediment trap / slope / Sieving
Jacoby Creek	*Lisle* [1986], *Lisle* [1989], data in *Almadeij* [2002], Wilcock and Kenworthy [2002] for diameters	HS (4.4 cm) / GS / Frozen core technique and sieving and Pebble count
Virgin Creek	*Andrews* [2000]	HS (7.62cm) / GS / random sampling of 1000 particles
Dupuyer Creek	*Whitaker and Potts [2007]*	Sed. Trap (1m high and 0.4m tall, 32-mm net mesh) / CM / Not specified. Only sediments coarser than 32 mm were captured and total bedload transport was estimated by *Whitaker and Potts [2007]* to be at least twice the reported values
Arbucies	*Batalla* [1997]	HS (7.62 cm), 0.45-mm net mesh / (GS?)/ Sieving. Bedload data given in submerged weight.
Elbow River	*Hollingshead* [1971]	Basket (60 cm wide) and VUV (45 cm wide) bedload samplers, Hydrophone, bed excavation / CM / Sieving
East Fork River	Years 1973–75 [*Leopold and Emmett*, 1976], year 1976 [*Leopold and Emmett*, 1977], year 1978 [*Leopold and Emmett*, 1997], year 1979 [*Emmett et al.*, 1980]	Bedload trap with endless belt, HS / GS /Sieving Bedload data given in submerged weight.
Borgne d'Arolla	*Gomez*[1988]	HS (7.6 cm), 0.5 mm net mesh / CM and slope measurement / Sampling with adhesive pad
Wind River	*Smalley et al.* [1994]	HS (size not specified)/ GS / Sieving
Snake and Clearwater River 1972–79	*Emmett and Seitz* [1974], *Seitz* [1976], *Jones and Seitz* [1980]	HS (7.6 and 15 cm) / GS /Pebble count and Sieve analyses
Little Granite Creek, Saint-Louis Cr., Fool Cr., Hayden Cr.	*Ryan et al*. [2002] http://www.fs.fed.us/rm/data_archive/dataaccess/contents_programarea.shtml	HS (7.6 cm) / GS / Pebble count
Ebro River	*Vericat et al.* [2006]	HS (7.6 and 15.2 cm) / GS / Bed sampling
**See the river list	*Williams and Rosgen* [1989]	These data result from a compilation of several studies; consequently several methods were used. HS (7.62 cm)/ GS or CM / generally dry sieving except for Colorado streams

* The format used is: Bedload / Hydraulic / Grain size distribution

ECM: Electromagnetic current meter; HS (7.6 cm): Helley-Smith 7.6-cm square entrance; GS: gauging station; CM: current meter

**River and stream data compiled by *Williams and Rosgen* [1989] and used in this study are from Alaska (Susitna River near Talkeetna, Talkeetna River near Talkeetna, Chulitna River below Canyon near Talkeetna, Susitna River at Sunshine, Tanana River at Fairbanks), Washington (Toutle River at Tower Road near Silver Lake, North Fork Toutle River near Kid Valley), Wyoming (Muddy Creek near Pinedale), Colorado (Yampa River at Deerlodge Park, Fourmile Creek near Fairplay, Mad Creek near Empire, Middle Fork Boulder Creek at Nederland, Jefferson Creek at Jefferson, Craig Creek near Bailey, Pony Creek near Antero Reservoir, Trail Creek near Westcreek, Blue River below Green Mountain Reservoir, Williams Fork near Leal, Upper South Fork Williams near Leal, Lower South Fork Williams Fork near Leal, Kinney Creek near Leal, Rich Creek near Weston Pass), Wisconsin (Wisconsin River at Muscoda, Black River near Galesville, Chippewa River near Caryville, Chippewa River at Durand, Chippewa River near Pepin).

Table 2: Main characteristics of additional rivers

	D_{16}	D_{50}	D_{84}	D_{90}	S	W	Nb**	% [0.1 < qs_{cal}/qs_{meas} <10]			
	mm	Mm	mm	mm	m/m	M		MPM	Park.	Schok.	Eq.12
Big wood River	28	116	250	380	0.0091	12.7	100	0	40	9	99
Blackmare Creek	26	95	220	252	0.03	10	88	0	5	0	91
Boise River	4	70	141	160	0.0038	53	82	0	44	20	100
Cat Spur Creek	13	27	73	80	0.011	4.9	35	0	17	0	46
Dollar Creek	6	74	145	171	0.0146	10	85	0	20	0	99
Egger Creek	2	22.8	122	164	0.0718	0.71	137	1	0	0	84
Fourth of July Creek	26	51	110	137	0.0202	7	77	0	5	0	77
Hawley Creek	15	40	100	140	0.0233	5	85	0	1	0	82
Herd Creek	37	67	107	122	0.0077	7.7	72	0	7	0	47
Johns Creek	48	207	558	1080	0.0207	12	34	0	0	0	30
Johnson Creek	98	190	380	430	0.004	22	72	0	0	0	97
Little Buckhorn Creek	4	78	207	298	0.0509	3	78	0	0	0	91
Little Slate Creek	97	207	380	450	0.0268	12	157	0	11	0	81
Lochsa River*	60	148	245	320	0.0023	72	72	0	3	0	96
Lolo Creek*	43	90	140	150	0.0097	11	89	0	8	0	88
Main Fork Red River	44	68	93	110	0.0059	10	198	0	8	0	66
Marsh Creek*	36	56	128	162	0.006	20	98	0	11	0	94
Middle Fork Salmon	48	144	288	360	0.0041	65	64	0	31	3	89
North Fork Clearwater	2	60	270	330	0.0005	75	72	0	0	3	80
Rapid River	47	94	170	180	0.0108	13	191	0	19	2	86
Salmon R bl Yankee	31	104	276	400	0.0034	34	60	0	10	0	90
Salmon R nr Obsidian	18	61	128	148	0.0066	13	50	0	74	30	100
Salmon R nr Shoup	20	95	174	205	0.0015	85	60	0	0	0	70
Squaw Creek (USGS)	20	43	72	82	0.01	6.5	92	0	23	2	92
Selway River*	75	200	265	310	0.0021	82	72	0	0	0	94
South Fork Red River*	44	86	150	165	0.0146	11	200	0	21	0	82
South Fork Salmon	2	38	76	113	0.0025	33	130	0	47	27	92
South Fork Payette*	16	55	150	175	0.004	50	72	0	11	0	65
Squaw Creek (USFS)	4	27	62	74	0.024	2.5	42	2	0	0	29
Thompson Creek	43	66	110	130	0.0153	6	81	0	44	0	96
Trapper Creek*	23	67	122	138	0.0414	5.7	166	0	10	0	82
Valley Creek*	11	63	160	200	0.004	41	192	0	1	0	80
West Fork Buckhorn	12	180	510	750	0.032	9	85	0	18	0	81
ALL DATA							3200	0	15	3	83

* *Two grain size distributions for the study period*

** *Number of bedload samples*

Table 3: Scores (%) in the ranges [0.1<$r = qs_{calculated}/qs_{measured}$<10] for each model tested with the *King et al.* [2004] data

	D_{16}	D_{50}	D_{84}	D_{90}	S	W	Nb	% [0.1 < qs_{cal}/qs_{meas} <10]

	mm	Mm	mm	mm	m/m	m		MPM	Park .	Schok	Eq.12
Oak Creek	19	54	80	86	0.01	3.7	119	0	14	3	71
Sagehen	21	58	104	130	0.011	2.6	55	0	56	5	98
Goodwin Creek	1	11.7	30	34	0.0025	12.9	358	4	53	55	75
Nahal Yatir	2	6	13	17	0.009	3.5	74	100	100	100	100
Jacoby Creek	2	27	95	104	0.0063	17.2	100	6	38	42	94
Virgin River	5	25	80	100	0.004	7.8	37	0	11	0	65
Dupuyer Creek	14	40	90	105	0.01	8.0	120	27	33	42	93
Arbucies	5	2.2	20	30	0.0095	6.3	40	48	3	33	58
Elbow River	7	30	80	100	0.0075	43.0	24	96	71	92	92
East Fork	0.3	1.3	13	25	0.0007	14.6	184	64	46	96	92
Borgne d'Arolla	4.5	11	20	33	0.03	1.8	31	77	74	97	81
Snake River	20	54	115	140	0.001	180.6	63	5	41	40	70
North Fork Clear.	1	20	70	140	0.0002	140.0	78	4	41	49	86
Wind River	0.6	17	50	73	0.001	41.0	25	72	88	96	100
Little Granite Cr	48	99	220	270	0.019	9.0	123	0	12	4	88
E. St. Louis Cr.	14	51	142		0.059	2.9	109	0	0	0	83
Fool Creek	11	38	100		0.053	1.9	95	0	0	0	85
Saint Louis 1	27	129	362		0.021	6 .7	98	0	24	1	74
Saint Louis 2	34	76	172		0.011	7.2	117	0	9	0	86
Saint Louis 3	34	82	181		0.019	8.3	107	0	19	2	96
Saint Louis 4	36	91	185		0.016	6.9	209	0	36	3	97
Saint Louis 4a	23	79	167		0.015	8.1	189	0	32	2	97
Saint Louis 5	30	146	543		0.05	5.3	93	0	0	0	99
Hayden Creek	20	68	140		0.025	5.4	76	0	7	3	100
Ebro River	20	39	70	86	0.0008	120	46	0	48	41	87
Susitna River near Talkeetns.	34	52	96	110	0.0016	182	39	0	31	18	92
Chultinana R below canyon	2	12	52	62	0.001	118	43	91	84	88	84
Sustina River at Sunshine	12	42	88	106	0.0018	158	41	2	59	83	93
Tanana River at Fairbanks	1	13	30	38	0.0005	311	50	32	96	94	100
Toutle River at Tower road	0.45	2	16	22	0.0026	52	28	82	61	79	71
N F Toutle R. - Kid Valley	0.6	2.5	20	25	0.0042	36	10	90	80	100	100
Muddy Creek near Pinedale	0.4	0.8	2	2.8	0.0012	4.6	21	86	67	100	100
Yampa R. at Deerlodge Park	0.3	0.6	1.5	1.8	0.0005	90	29	100	72	100	83
Fourmile Creek near Fairplay	7	48	190	240	0.016	3.4	18	0	0	0	67
Mad Creek near Empire	80	220	460	500	0.0856	1.9	16	0	0	0	31
Middle Fork of Boulder Cr.	15	70	200	235	0.0163	17	14	0	0	0	64
Jefferson Cr. near Jefferson	1	30	112	140	0.016	4	12	0	0	0	42
Craig Cr. near Baileyn Colo	10	160	450	520	0.023	6.5	22	0	0	0	45
Pony Creek near Antero Res.	0.16	2.5	6	9	0.005	1.1	14	7	0	0	43
Trail Creek near WestCreek	0.5	2.7	7.5	10.5	0.018	2.8	13	23	0	8	8
Blue R. Green Mount. Reser.	4	58	220	258	0.0026	34	12	0	0	0	100
Williams Fork near Leal	8	28	86	110	0.0058	17.8	19	0	37	11	58
Upper South Fork of Wil. F.	8	22	56	62	0.0096	9.5	11	0	27	9	91
Lower South Fork of Wil. F.	10	72	224	280	0.016	9	16	0	6	0	88
Kinney creek near Leal	20	56	200	242	0.019	4.9	16	0	0	6	81
Rich Creek near Weston Pass	2	56	220	280	0.039	4.4	16	0	0	0	100
Wisconsin River at Muscoda	0.18	0.42	0.95	1.1	0.0003	287	20	100	80	95	100
Black River near Galesville	0.25	0.45	0.9	1	0.0002	104	17	47	100	88	100
Chippewa R. near Caryville	0.45	4.5	20	24	0.0002	226	9	22	78	78	100
Chippewa river at Durand	0.31	0.65	4	10	0.0003	205	25	72	76	100	100
Chippewa river near Pepin	0.3	0.5	1	1.3	0.0003	240	18	100	83	100	100
ALL DATA							3119	17	35	33	86

Table 4: Scores (%) in the ranges [$0.1 < r = qs_{calculated}/qs_{measured} < 10$] for each model tested with the data presented in Table 2 (Blind test)

Model (all data, 6319 field values)	$0.5 < r < 2$	$0.2 < r < 5$	$0.1 < r < 10$
Meyer-Peter and Mueller	3	7	9
Parker	7	17	25
Schoklitsch	6	14	18
This study (Eq.12)	36	70	85

Table 5: Scores (%) for each model tested on the entire field data set (6319 values)

Model tested on data of Table 2	Phase 1 (1754 values)	Phase 2 (769 values)	Phase 3 (596 values)
Meyer-Peter and Mueller	0	22	68
Parker	24	44	63
Schoklitsch	6	54	89
This study (Eq.12)	88	79	89

Table 6: Scores (%) for each model and for each phase of transport

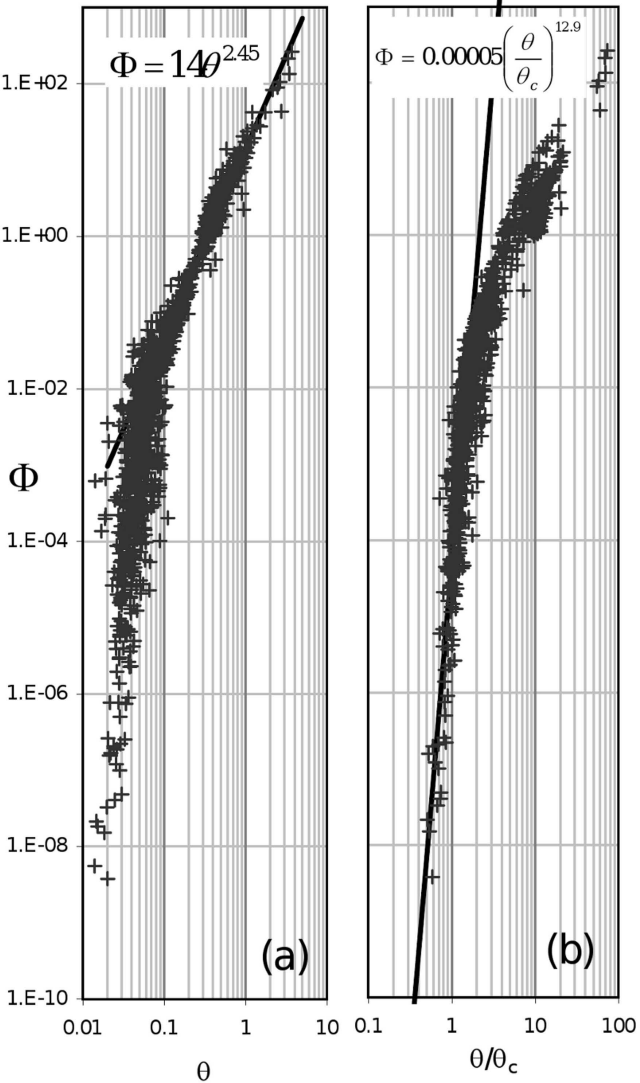
$\Phi = 14\theta^{2.45}$
$\Phi = 0.00005\left(\frac{\theta}{\theta_c}\right)^{12.9}$
1.E+02
1.E+00
1.E-02
1.E-04
1.E-06
1.E-08
1.E-10
Φ
0.01
0.1
1
10
θ
(a)
0.1
1
10
100
θ/θc
(b)

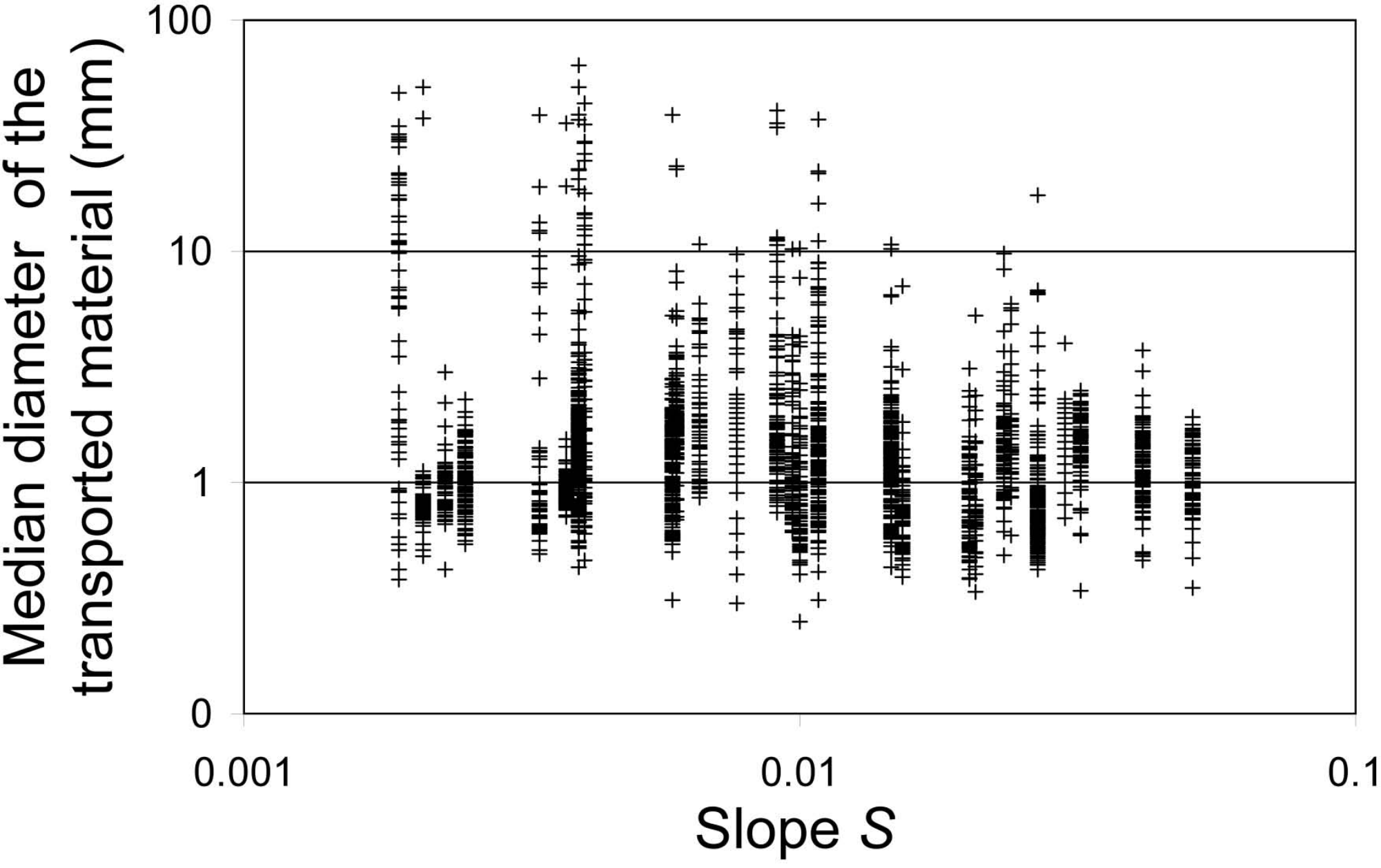
Median diameter of the transported material (mm)
100
10
1
0
0.001
0.01
0.1
Slope S

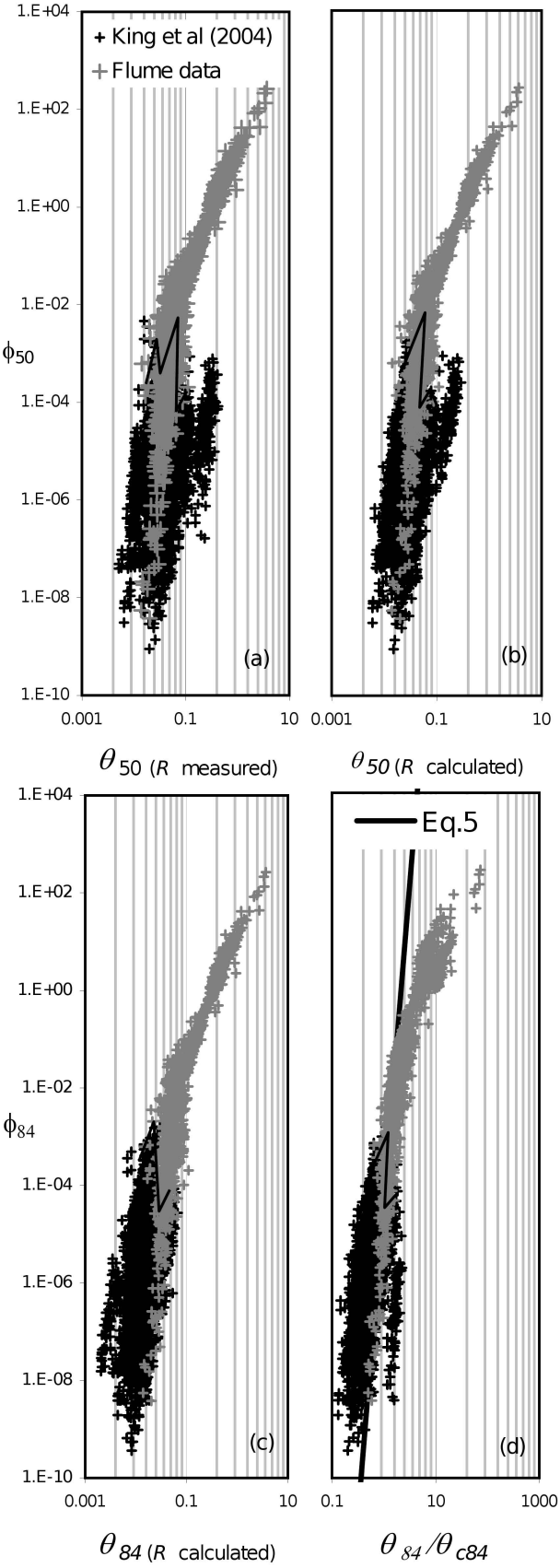
King et al (2004)
Flume data
1.E+04
1.E+02
1.E+00
1.E-02
1.E-04
1.E-06
1.E-08
1.E-10
ϕ50
0.001
0.1
10
(a)
(b)
θ50 (R measured)
θ50 (R calculated)
ϕ84
(c)
(d)
Eq.5
0.1
1000
θ84 (R calculated)
θ84/θc84

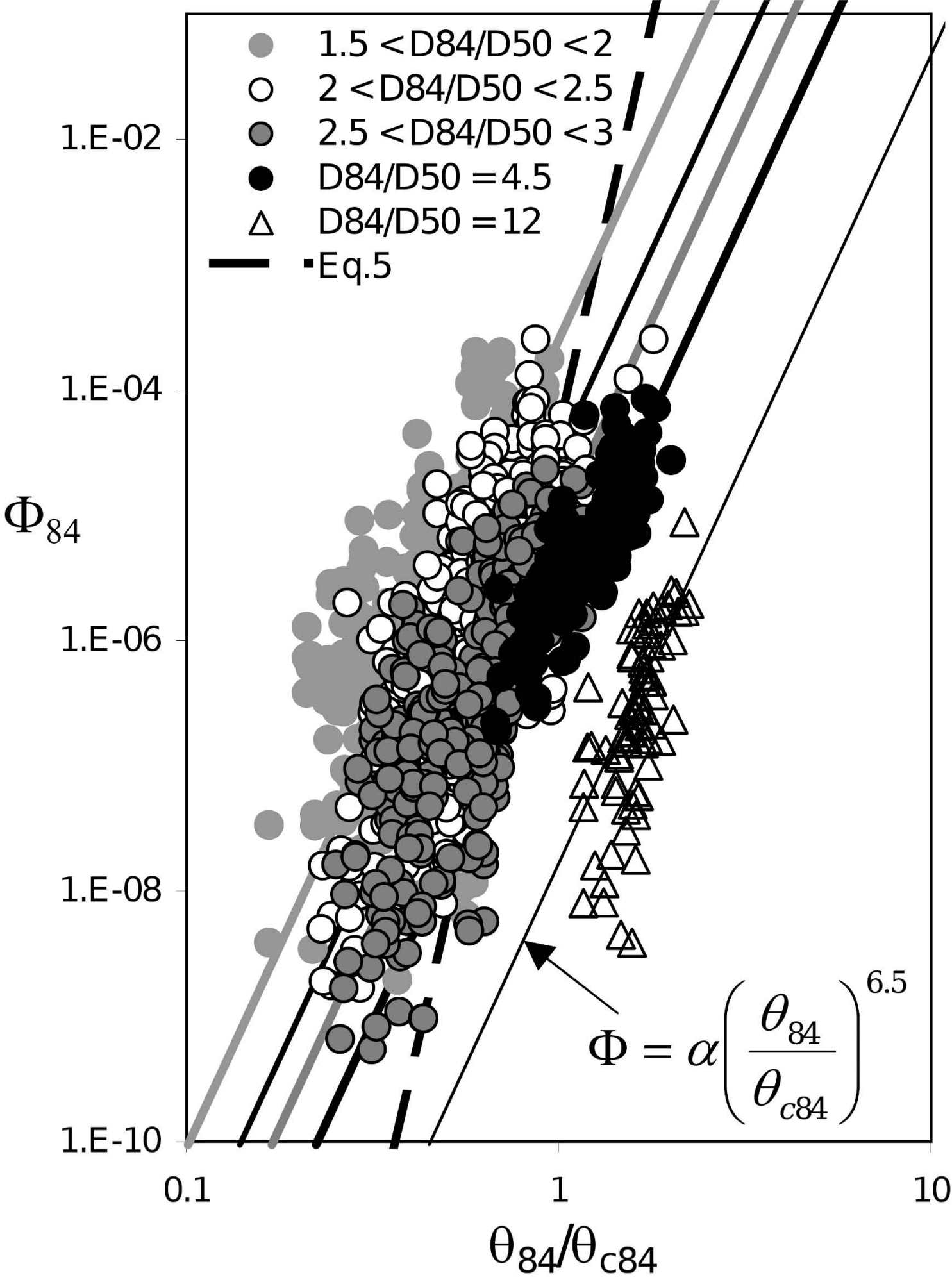
1.5 < D84/D50 < 2
2 < D84/D50 < 2.5
2.5 < D84/D50 < 3
D84/D50 = 4.5
D84/D50 = 12
Eq.5
1.E-02
1.E-04
1.E-06
1.E-08
1.E-10
Φ84
0.1
1
10
θ84/θc84
$\Phi = \alpha \left(\frac{\theta_{84}}{\theta_{c84}} \right)^{6.5}$

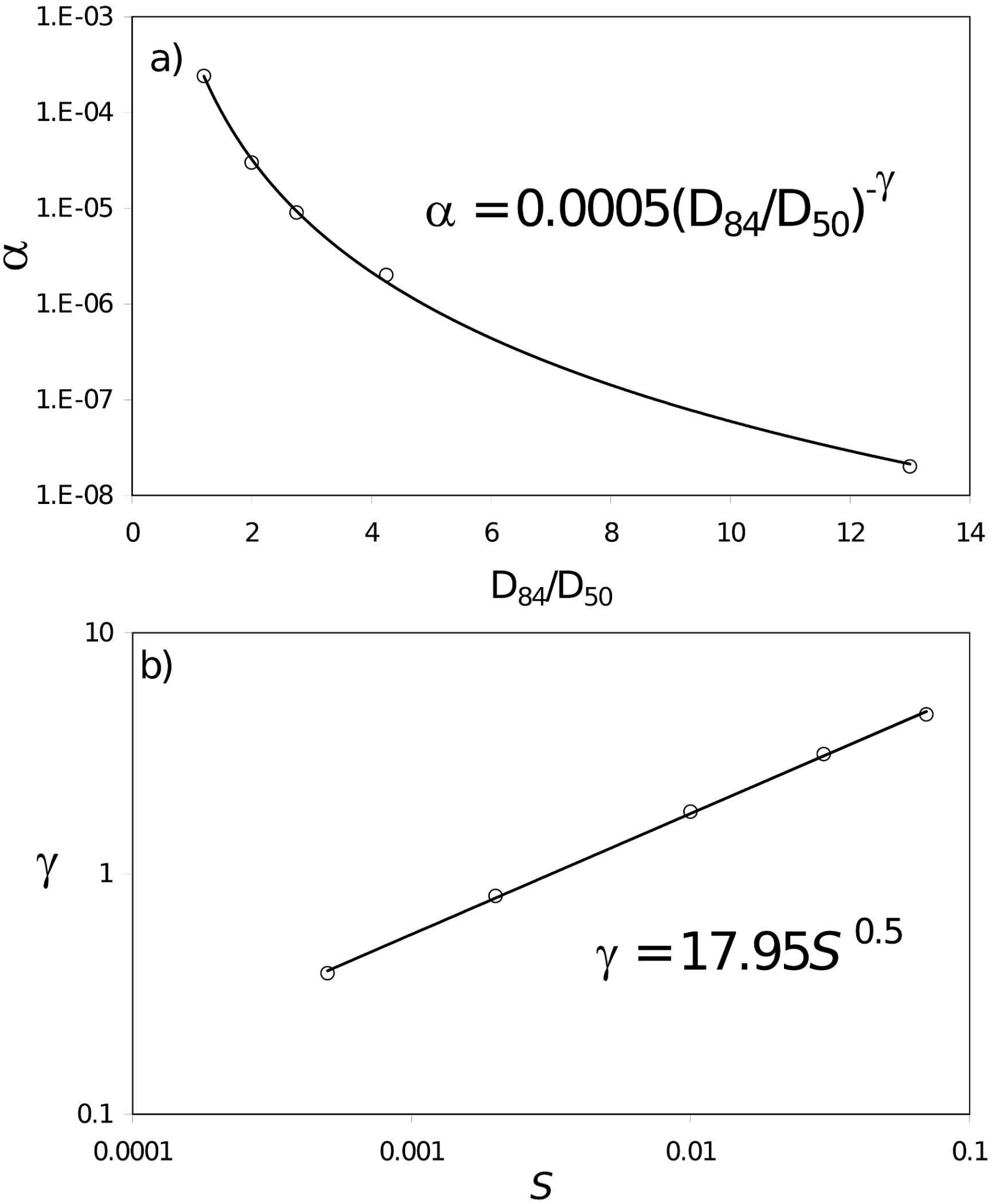
a)
1.E-03
1.E-04
1.E-05
1.E-06
1.E-07
1.E-08
α
0
2
4
6
8
10
12
14
D84/D50
α =0.0005(D84/D50)-γ
b)
10
1
0.1
γ
0.0001
0.001
0.01
0.1
S
γ =17.95S 0.5

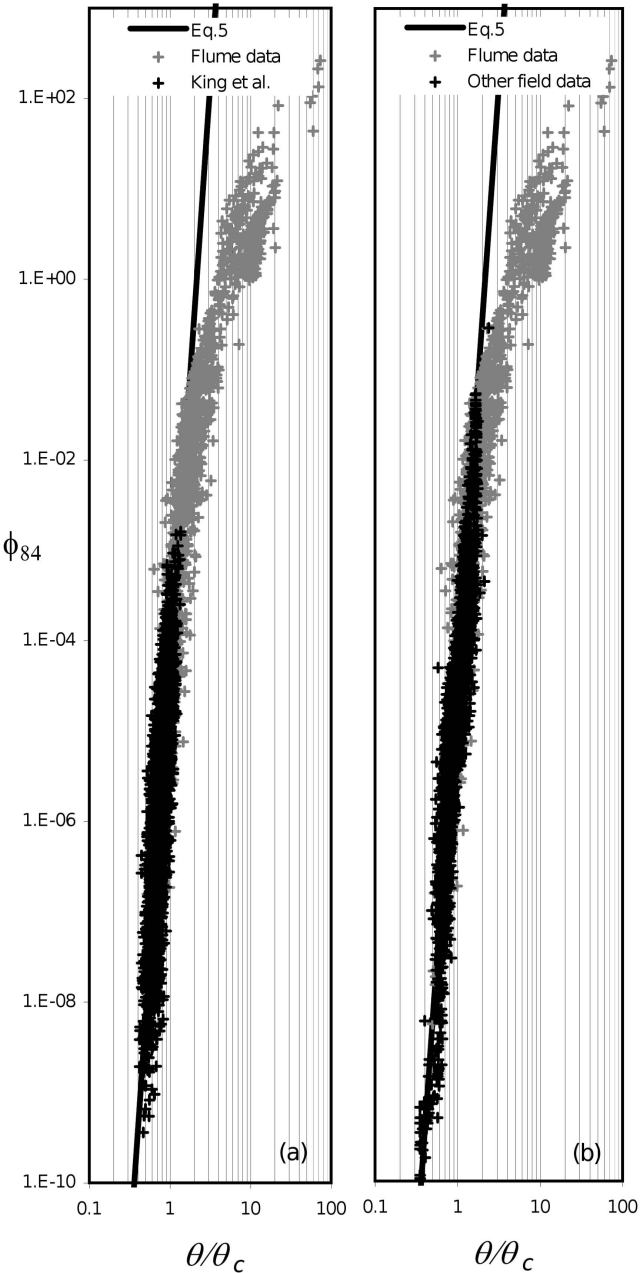
Eq.5
Flume data
King et al.
Eq.5
Flume data
Other field data
1.E+02
1.E+00
1.E-02
1.E-04
1.E-06
1.E-08
1.E-10
ϕ_{84}
0.1
1
10
100
θ/θ_c
(a)
(b)

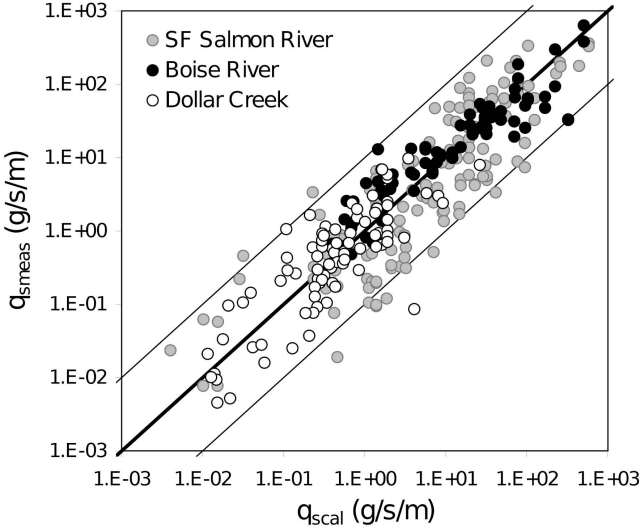
SF Salmon River
Boise River
Dollar Creek
1.E+03
1.E+02
1.E+01
1.E+00
1.E-01
1.E-02
1.E-03
q_{smeas} (g/s/m)
1.E-03
1.E-02
1.E-01
1.E+00
1.E+01
1.E+02
1.E+03
q_{scal} (g/s/m)

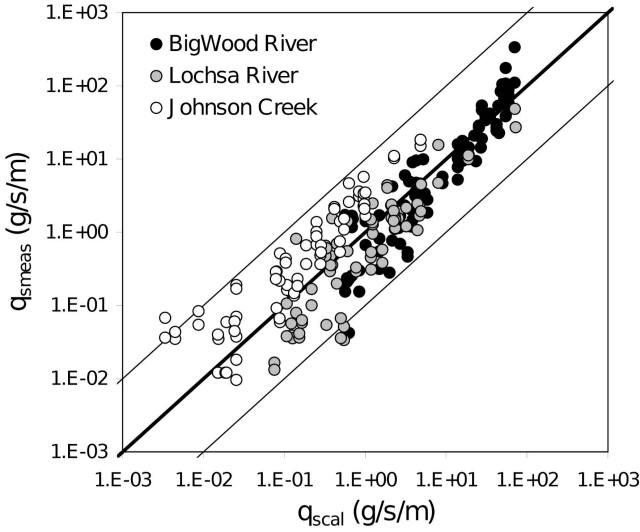
BigWood River
Lochsa River
Johnson Creek
1.E+03
1.E+02
1.E+01
1.E+00
1.E-01
1.E-02
1.E-03
q_{smeas} (g/s/m)
1.E-03
1.E-02
1.E-01
1.E+00
1.E+01
1.E+02
1.E+03
q_{scal} (g/s/m)

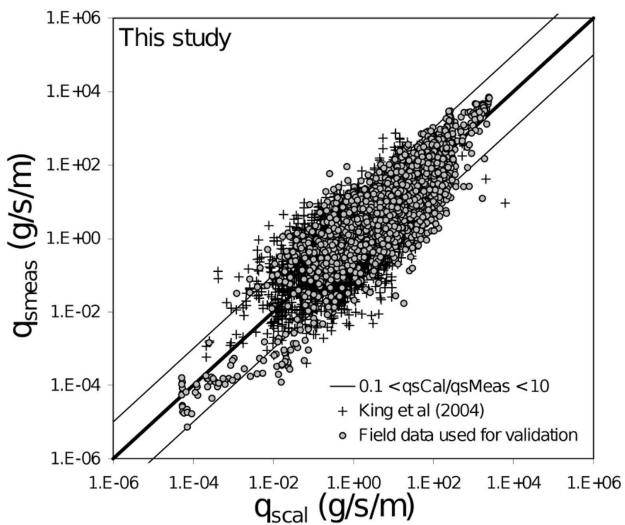
This study
1.E+06
1.E+04
1.E+02
1.E+00
1.E-02
1.E-04
1.E-06
qsmeas (g/s/m)
1.E-06 1.E-04 1.E-02 1.E+00 1.E+02 1.E+04 1.E+06
qscal (g/s/m)
0.1 <qsCal/qsMeas <10
King et al (2004)
Field data used for validation

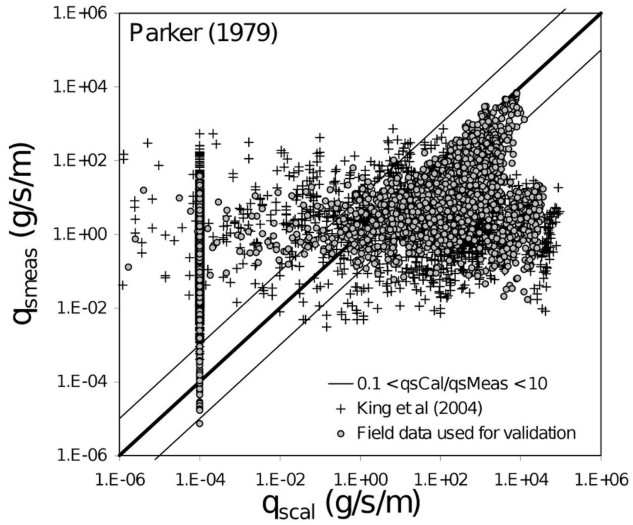
Parker (1979)
1.E+06
1.E+04
1.E+02
1.E+00
1.E-02
1.E-04
1.E-06
qsmeas (g/s/m)
1.E-06 1.E-04 1.E-02 1.E+00 1.E+02 1.E+04 1.E+06
qscal (g/s/m)
0.1 <qsCal/qsMeas <10
King et al (2004)
Field data used for validation

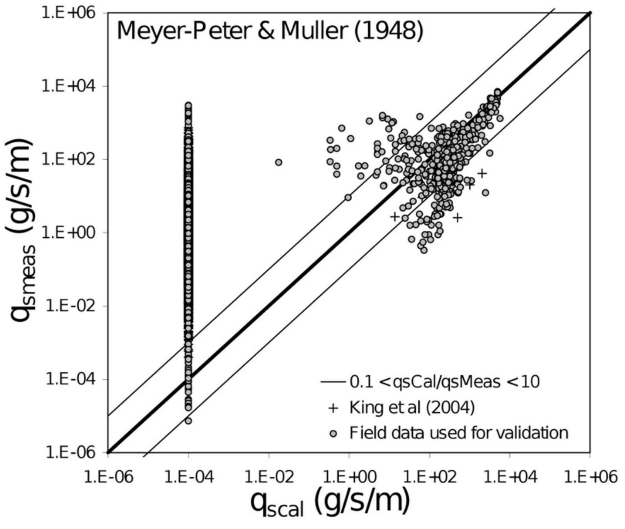
Meyer-Peter & Muller (1948)
1.E+06
1.E+04
1.E+02
1.E+00
1.E-02
1.E-04
1.E-06
qsmeas (g/s/m)
1.E-06 1.E-04 1.E-02 1.E+00 1.E+02 1.E+04 1.E+06
qscal (g/s/m)
0.1 <qsCal/qsMeas <10
King et al (2004)
Field data used for validation

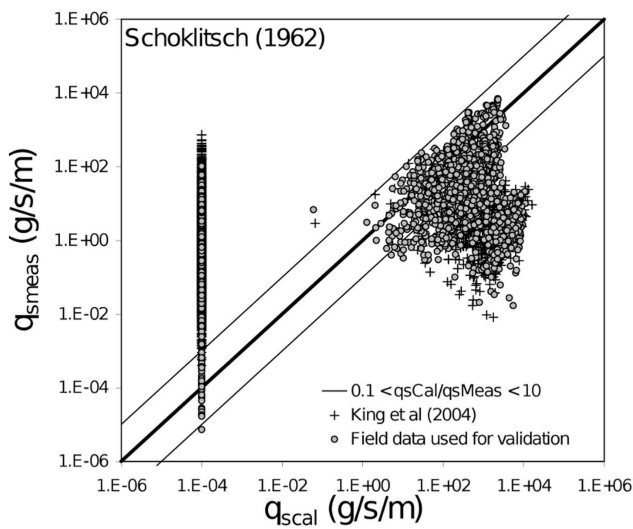
Schoklitsch (1962)
1.E+06
1.E+04
1.E+02
1.E+00
1.E-02
1.E-04
1.E-06
qsmeas (g/s/m)
1.E-06 1.E-04 1.E-02 1.E+00 1.E+02 1.E+04 1.E+06
qscal (g/s/m)
0.1 <qsCal/qsMeas <10
King et al (2004)
Field data used for validation

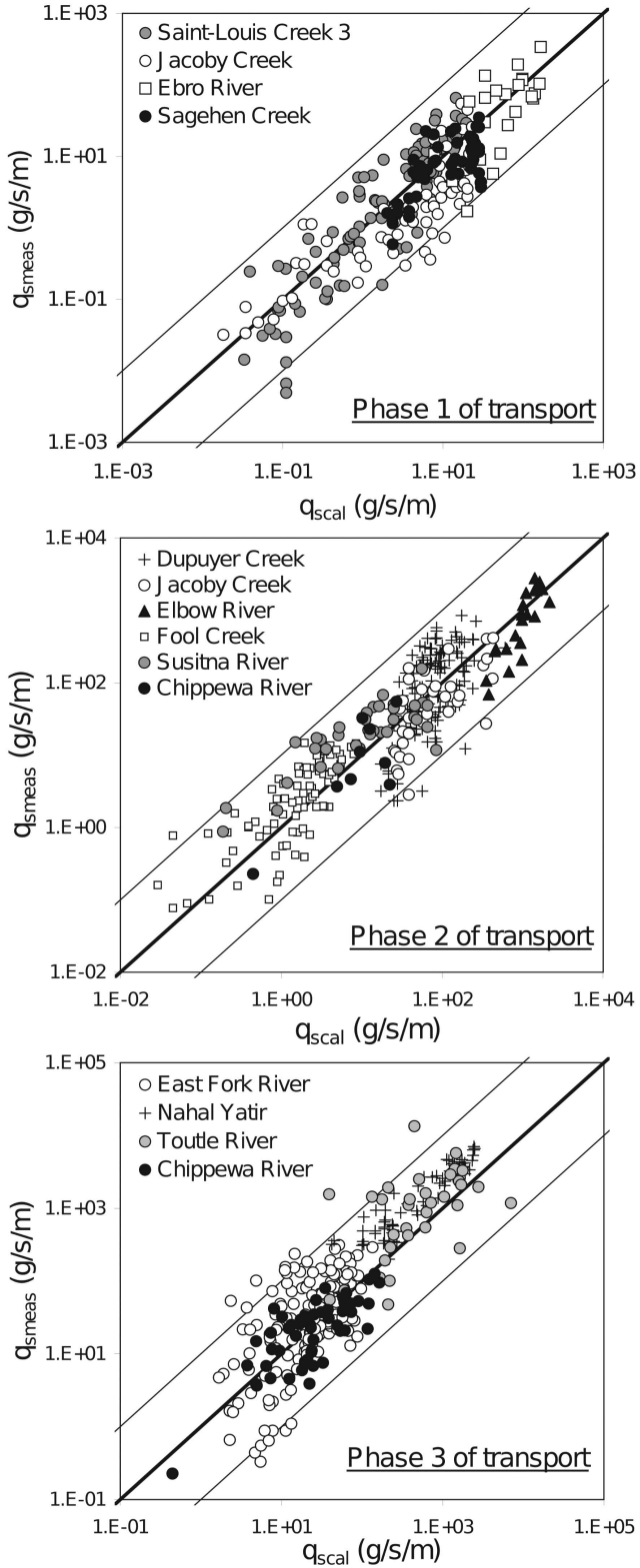
Saint-Louis Creek 3
Jacoby Creek
Ebro River
Sagehen Creek
Phase 1 of transport
1.E+03
1.E+01
1.E-01
1.E-03
1.E-03
1.E-01
1.E+01
1.E+03
qsmeas (g/s/m)
qscal (g/s/m)
Dupuyer Creek
Jacoby Creek
Elbow River
Fool Creek
Susitna River
Chippewa River
Phase 2 of transport
1.E+04
1.E+02
1.E+00
1.E-02
1.E-02
1.E+00
1.E+02
1.E+04
qsmeas (g/s/m)
qscal (g/s/m)
East Fork River
Nahal Yatir
Toutle River
Chippewa River
Phase 3 of transport
1.E+05
1.E+03
1.E+01
1.E-01
1.E-01
1.E+01
1.E+03
1.E+05
qsmeas (g/s/m)
qscal (g/s/m)

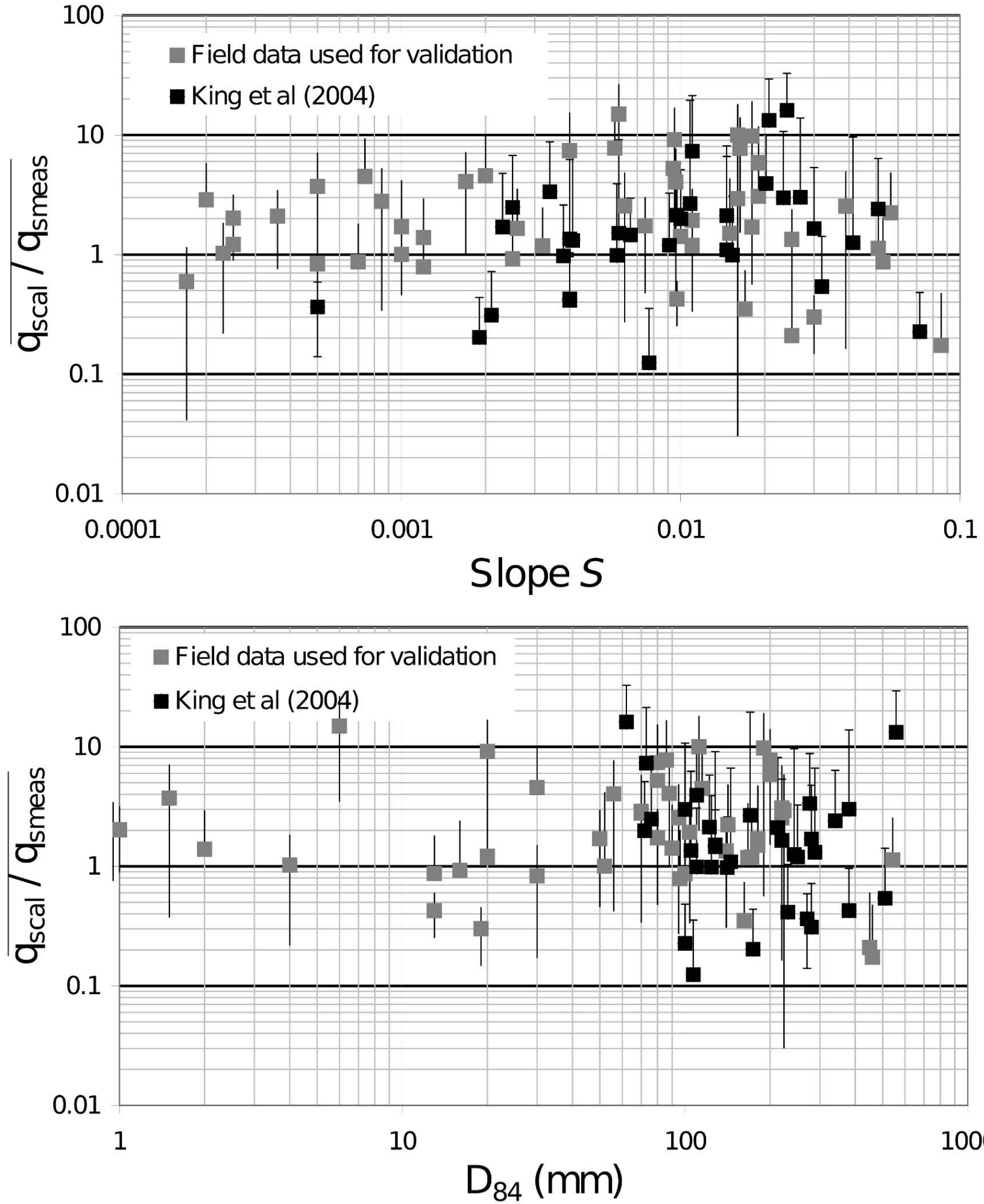
Field data used for validation
King et al (2004)
100
10
1
0.1
0.01
$\overline{q_{scal}} / q_{smeas}$
0.0001
0.001
0.01
0.1
Slope S
Field data used for validation
King et al (2004)
100
10
1
0.1
0.01
$\overline{q_{scal}} / q_{smeas}$
1
10
100
1000
D_{84} (mm)

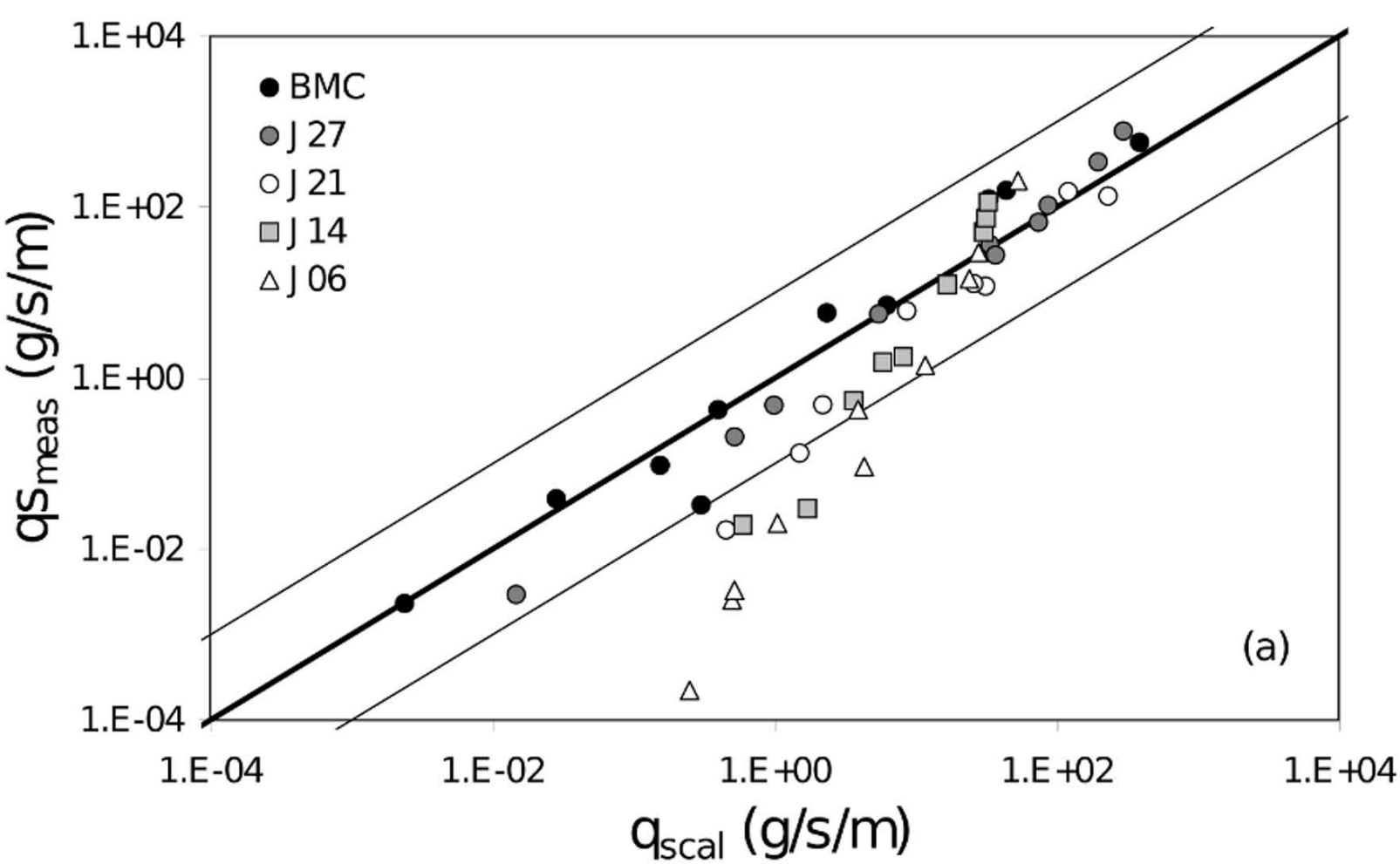
1.E+04
1.E+02
1.E+00
1.E-02
1.E-04
qs$_{meas}$ (g/s/m)
BMC
J 27
J 21
J 14
J 06
(a)
1.E-04
1.E-02
1.E+00
1.E+02
1.E+04
q$_{scal}$ (g/s/m)

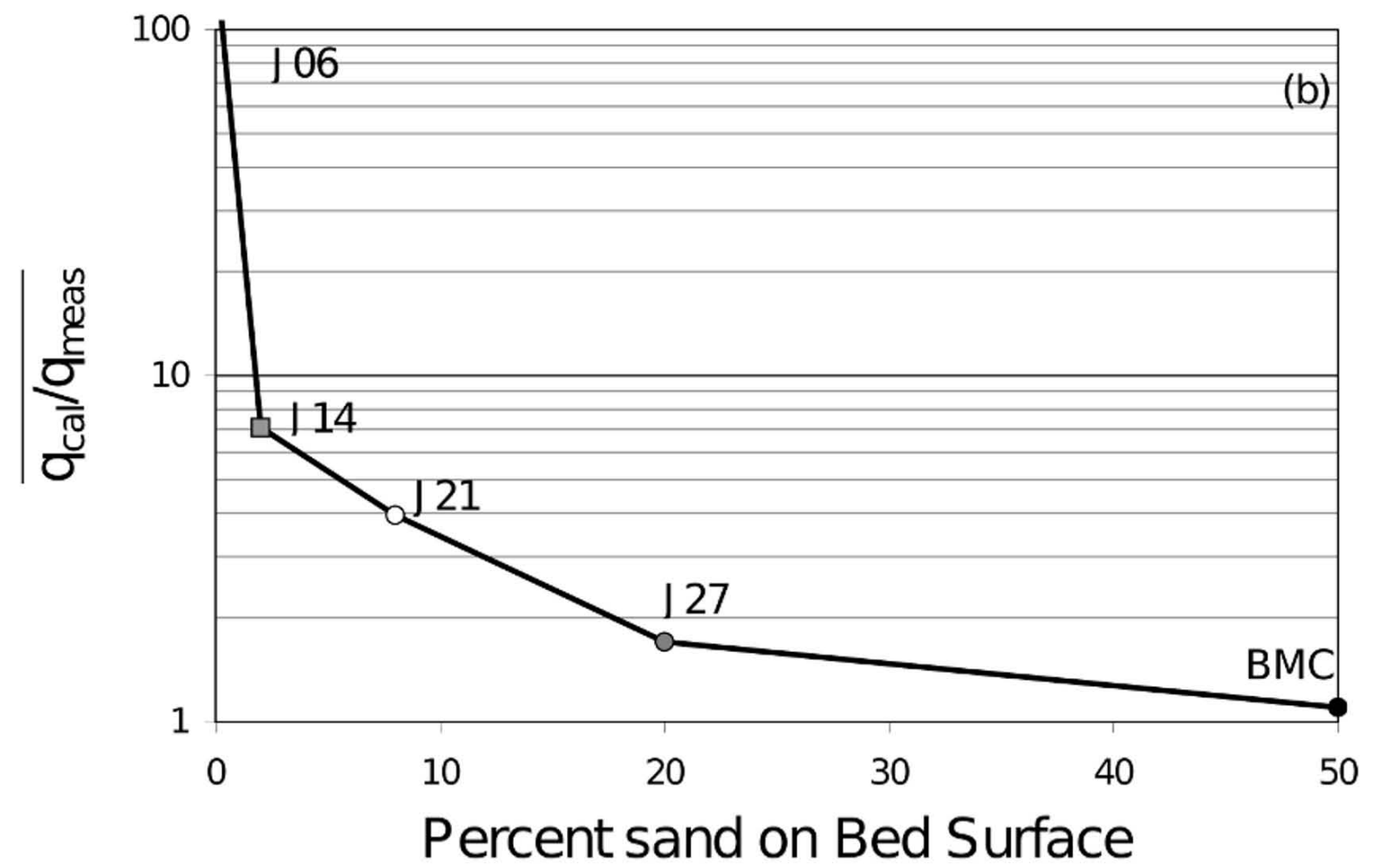
100
10
1
$\overline{q_{cal}/q_{meas}}$
J 06
(b)
J 14
J 21
J 27
BMC
0
10
20
30
40
50
Percent sand on Bed Surface

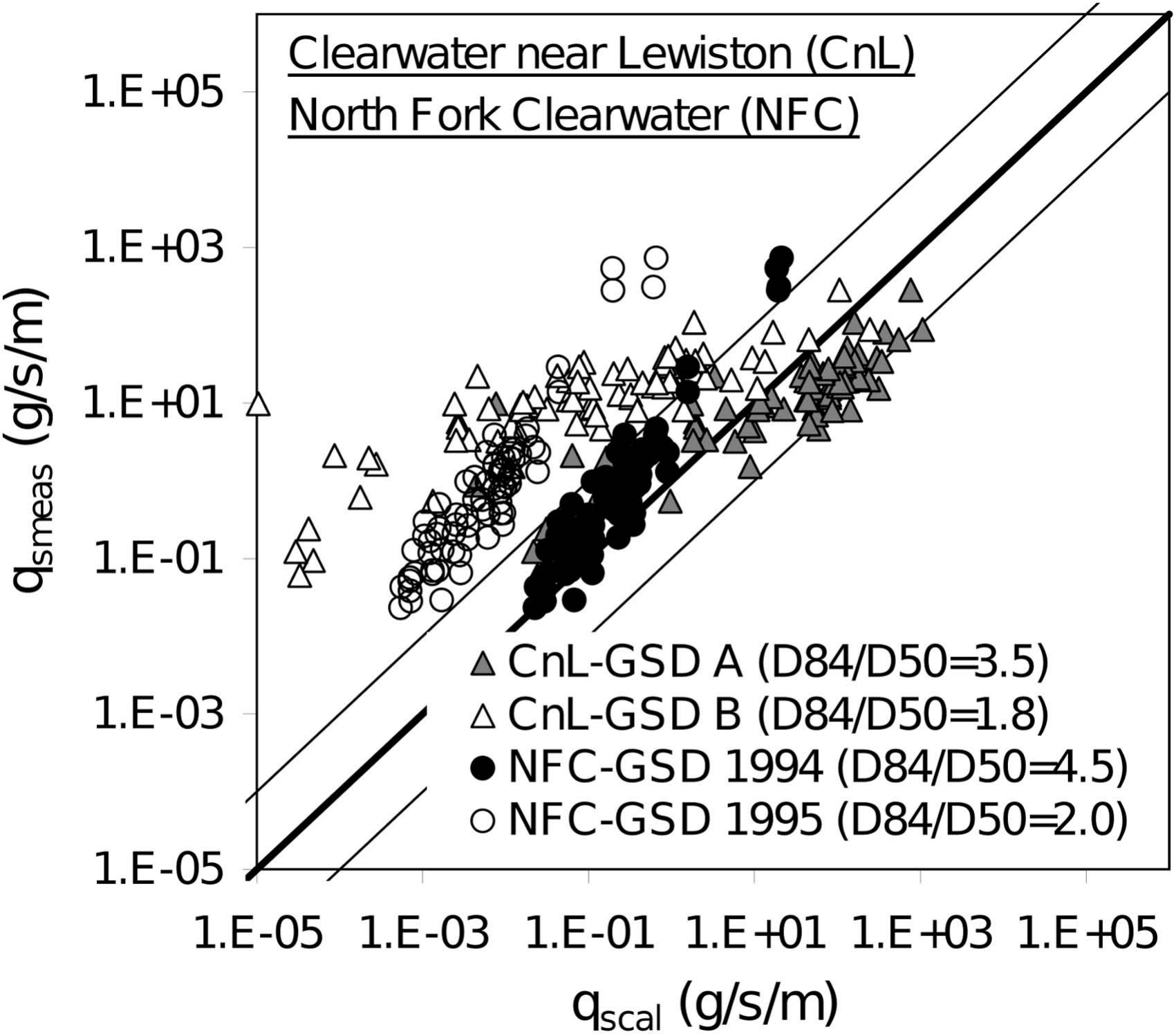
Clearwater near Lewiston (CnL)
North Fork Clearwater (NFC)
CnL-GSD A (D84/D50=3.5)
CnL-GSD B (D84/D50=1.8)
NFC-GSD 1994 (D84/D50=4.5)
NFC-GSD 1995 (D84/D50=2.0)
1.E+05
1.E+03
1.E+01
1.E-01
1.E-03
1.E-05
1.E-05
1.E-03
1.E-01
1.E+01
1.E+03
1.E+05
q_{smeas} (g/s/m)
q_{scal} (g/s/m)